CERTIFICATE OF RESEARCH

The thesis title **"PERFORMANCE EVALUATION OF WAVE-CARPET IN WAVE ENERGY EXTRACTION AT DIFFERENT COASTAL REGIONS: AN ANALYTICAL APPROACH"** submitted by **SAJIA MISKATI (160011054), FARIHANA MUMTAHIN FARIN (160011027)** has been accepted as satisfactory in partial fulfillment of the requirement for the Degree of Bachelor of science in Mechanical Engineering on March 2021.

Signature of the Supervisor

01/03/2021

Dr. Mohammad Ahsan Habib
Professor
Department of Mechanical & Production Engineering (MPE)
Islamic University of Technology (IUT), OIC

Candidate's Declaration

It is hereby declared that this thesis or any part of it has not been submitted elsewhere for the award of any degree or diploma.

Signature of the Candidates'

Sajia Miskati 01.03.21

Sajia Miskati

Student No: 160011054

Farhana Mumtahin Farin (01.03.21)

Farhana Mumtahin Farin

Student No: 160011027

Department of Mechanical and Production Engineering (MPE)
Islamic University of Technology (IUT), OIC
Board Bazar, Gazipur
Dhaka, Bangladesh.

Signature of the Supervisor

01/03/2021

Dr. Mohammad Ahsan Habib
Professor
Department of Mechanical & Production Engineering (MPE)
Islamic University of Technology (IUT), OIC

ISLAMIC UNIVERSITY OF TECHNOLOGY (IUT)

PERFORMANCE EVALUATION OF WAVE-CARPET IN WAVE ENERGY EXTRACTION AT DIFFERENT COASTAL REGIONS: AN ANALYTICAL APPROACH

B.Sc. Engineering (Mechanical) THESIS

BY

SAJIA MISKATI, FARHANA MUMTAHIN FARIN

Department of Mechanical and Production Engineering

Islamic University of Technology (IUT), OIC

MARCH 2021

PERFORMANCE EVALUATION OF WAVE-CARPET IN WAVE ENERGY EXTRACTION AT DIFFERENT COASTAL REGIONS: AN ANALYTICAL APPROACH

BY

SAJIA MISKATI (160011054), FARHANA MUMTAHIN FARIN (160011027)

A THESIS PRESENTED TO THE DEPARTMENT OF MECHANICAL AND PRODUCTION ENGINEERING, ISLAMIC UNIVERSITY OF TECHNOLOGY DHAKA IN PARTIAL FULFILMENT OF THE REQUIREMENT FOR THE AWARD OF DEGREE FOR

BACHELOR OF SCIENCE (B. Sc.) IN MECHANICAL ENGINEERING

MARCH 2021

Certificate of Research

The thesis title **"PERFORMANCE EVALUATION OF WAVE-CARPET IN WAVE ENERGY EXTRACTION AT DIFFERENT COASTAL REGIONS: AN ANALYTICAL APPROACH"** submitted by **SAJIA MISKATI (160011054), FARHANA MUMTAHIN FARIN (160011027)** has been accepted as satisfactory in partial fulfillment of the requirement for the Degree of Bachelor of science in Mechanical Engineering on March 2021.

Signature of the Supervisor

Dr. Mohammad Ahsan Habib
Professor
Department of Mechanical & Production Engineering (MPE)
Islamic University of Technology (IUT), OIC

Candidate's Declaration

It is hereby declared that this thesis or any part of it has not been submitted elsewhere for the award of any degree or diploma.

Signature of the Candidates'

Sajia Miskati

Student No: 160011054

Farhana Mumtahin Farin

Student No: 160011027

Department of Mechanical & Production Engineering (MPE)
Islamic University of Technology (IUT), OIC
Board Bazar, Gazipur
Dhaka, Bangladesh.

Signature of the Supervisor

Prof Dr. Mohammad Ahsan Habib
Professor
Department of Mechanical & Production Engineering (MPE)
Islamic University of Technology (IUT), OIC

Acknowledgements

We would like to begin by saying Alhamdulillah and grateful to Almighty Allah who made it possible for us to finish this work successfully on time. Equally say a big thanks to our supervisor Dr. Mohammad Ahsan Habib, Professor, Department of Mechanical & Production Engineering, IUT and Tanvir Shahriar, Lecturer, Department of Mechanical & Production Engineering, IUT for all their support, ideas about experiments, discussions, time and for explaining so patiently the hard topics and checking this thesis and papers above all their valuable care and concern. These will ever remain in our memory. Thanks to our examiners for their constructive ideas, suggestions and double checking our work.

Table of Contents

List of Figures

List of Table

List of Symbols

$\boldsymbol{\rho}$	Density of fluid
$\boldsymbol{g}$	Gravity acceleration
$\boldsymbol{\eta_s}$	Surface elevation
$\boldsymbol{\eta_b}$	Bottom elevation
$\boldsymbol{\omega}$	Frequency of the wave
$\boldsymbol{\Omega}$	Dimensionless frequency
$\boldsymbol{\Omega_i}$	Imaginary part of dimensionless frequency
$\boldsymbol{\Omega_r}$	Real part of dimensionless frequency
$\boldsymbol{\zeta}$	Dimensionless damping ratio
$\boldsymbol{\gamma}$	Dimensionless restoring force
$\boldsymbol{\mu}$	Shallowness
$\boldsymbol{T}$	Wave period
$\boldsymbol{\alpha}$	Dimensionless amplitude ratio
$\boldsymbol{E_c}$	***Wave carpet*** energy extraction

K^*	Stiffness coefficient of the viscoelastic bottom per unit area
L	Wave length
D_d	Dimensionless constant
ϵ	Energy in dimensionless form
A_c	Area of the carpet
h	Depth of water level
k	Wave number of the propagating wave
H	Significant height
E_{tot}	Total energy
E_{pot}	Potential energy
E_{kin}	Kinetic energy
P_{wave}	Wave power
τ	Dimensionless time
a_s	Surface amplitude
a_b	Bottom amplitude
f	Frequency

b^*	Viscous damping coefficient
C_g	Group velocity of wave

Abstract

Globally, muddy seafloors have been reported to extract a significant percentage of energy in wave that interacts at different wavelengths. Since mud is capable of taking so much energy out of ocean waves, the researchers are planning to use this incredible concept to design an efficient Wave energy converter. They have proposed an idea of creating a viscoelastic carpet for Wave Energy Conversion (CWEC) mounting on coastal floors through a network of vertically oriented some springs and generators, which should extract wave energy exactly in the same way as the muddy seafloor does. Dynamic ripples and undulations can be induced on the surface of its spring and electrical power produced by these perturbations. This paper presents an analysis of performance of a mud-resembling carpet in harvesting ocean wave energy for multiple sea states in different countries. In addition, a brief on energy extraction using wave carpet technology for various locations with varying water depth and some recommendations for future studies are specially highlighted.

Chapter 1 Introduction

Humans forever have had the vision of using the continuous movement of oceans as an energy source to generate power. While these visions may seem unconvincing, we are slowly but steadily ascending the right steps to fulfill this visualization. Ocean energy technologies perhaps can meet the constantly increasing global energy demand with time. That is why many researchers and scientists are interested in finding numerous other ways of extracting energy from the ocean.

In recent years, some Governments and the European Commissions have undertaken remarkable work on wave energy and have contributed a number of new device designs, as well as modifications of existing ones [1]. Prof. Reza Alam from University of California (UC), Berkeley with his team has introduced a device which is called Wave Carpet, known as Magic Carpet as well, that not only consumes energy, but also transforms energy into usable energy. This paper however, explores the performance and feasibility of using wave carpet in harvesting ocean wave energy by measuring the incoming power to the carpet and energy extraction by the carpet for different coastal regions by analytical approach. The countries chosen for our study are Australia, Belgium, China, India and Italy.

1.1 Prospective Aspects of Wave Energy

Since wave energy is predictable [2], to use wave energy as a source of extracting power, provides significant advantages. Wave energy is a form of renewable energy (RE) with a high energy density and utilization factor than other renewable energy sources. Also, comparing to other green energy sources, it has a smaller environmental impact.

According to the research conducted by the International Energy Agency (IEA) [3], the oceans' overall energy capacity is projected to be about 93,100 TWh a year.

Depending on the Wave Energy Converter technology, the energy from the waves can be harnessed almost throughout the day [4] with a maximum extraction percentage of 90% [5], as opposed to significant lower numbers for solar and wind energy (30% and 20% respectively).

1.2 Environmental Aspects of Wave Energy

The demand for cleaner and greener forms of energy has pushed governments and researchers all around the world to investigate into the largely untapped renewable sector to fight against the increasing rate of greenhouse gasses (GHG's) that have surrounded the earth's atmosphere[1]. However, renewable technologies are regarded as environmentally friendly energy sources, which can minimize greenhouse effects as well as environmental impacts. This section points out a few advantages of wave energy and also outlines some of the disadvantages associated with wave energy.

- The Kyoto Protocol calls for a 50% cut in greenhouse gas emissions by 2050. Keeping this in consideration it can be said that renewable energy solutions provide a fantastic potential to reduce greenhouse gas emissions and global warming.
- We know that significant levels of CO_2 and CH_4 are produced during the combustion of fossil fuels, like coal, oil, gas etc. So one of the advantages of wave energy is, an estimation has been concluded[2] as for each MWh produced by ocean energy, 300 kg of CO_2 can be avoided.

– Another benefit of using wave energy is its impact on tourism. It is important to preserve a natural ecological landscape, which includes current historical monuments and appropriate tourism policies. Thus, establishment of wave energy in coastal regions would have a positive impact on its tourism industry[3].

Whenever one source of energy is converted into another, it inadvertently interrupts other issues. The installation and use of wave energy systems and strategies may also have an environmental impact in terms of coastal erosion, fishing industry, sedimentary flow, navigational hazards etc.

– It has some detrimental effects on aquatic, fish populations and nearshore intertidal and benthic habitats, large marine vertebrates (sea birds, marine mammals and large fish), oceanographic and coastal processes[3].
– It has been observed that some WEC's such as Oyster, generate noise pollution, as a result disturb aquatic life.
– Constructing large wind farms can cause damage to shore lines or coast line areas[2].

A summary[4] of the environmental effect of wave energy conversion technologies is shown .

Type of environmental effect	Rate of effect
Land use	Weak
Construction and maintenance	Weak
Coastal erosion	Weak–medium
Fish and Marine biota	Weak
Noise	Weak

Figure 1.1: Some environmental effects of WECs[2].

Also, authors in [5] explored some detrimental effects of wave farms is included for changing the fish population due to larvae transportation.

1.3 Wave Energy Converters

Wave energy can be harnessed by the application of special types of devices called wave energy converters (WEC). Wave energy converters can be in some specific system forms such as Oscillating Water Column (OWC), Archimedes Wave Swing, Oyster, hinged contour devices as the Pelamis, overtopping devices as the Wave Dragon and many more [6]. Extraction of energy can be occurred from the waves, tides, temperature gradients, salinity gradients currents and so on where wave energy is more persistent and predictable among all sources of energy [7]. There are many more than 1000 different patented wave energy converter proposals[8] and several have demonstrated the potential for commercial purposes. Also, over 200 different types of WEC's exist, with several still undergoing the testing phase[9]. However, there are a large number and wave variety of wave energy converters that is different in technological design and conceptions.

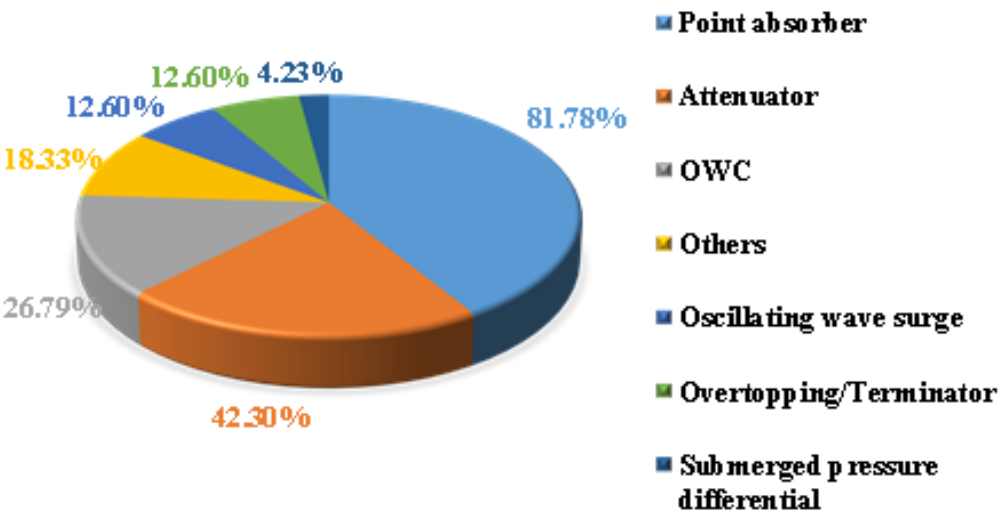

Figure 1.2: Wave energy converter development %.

1.3.1 Brief description of common types of WECs

Attenuator is a floating structure that operates in the same direction as the waves and essentially rides them. As the wave flows between the two arms, these instruments absorb energy from the relative motion of the two arms[11]. Basically, it is a long floating frame made up of several segments that floats parallel to the waves and functions similarly to a point absorber, flexing in response to varying wave heights. The segments then operate a hydraulic pump or another form of energy converter, which is connected to a power source. Electricity is then feed from a transformer held in the nose of the structure to a cable in the ocean floor to the shore to be put onto the grid [16]. One of the disadvantages of using this kind of device is it needs a large farm area to be a profitable proposition.

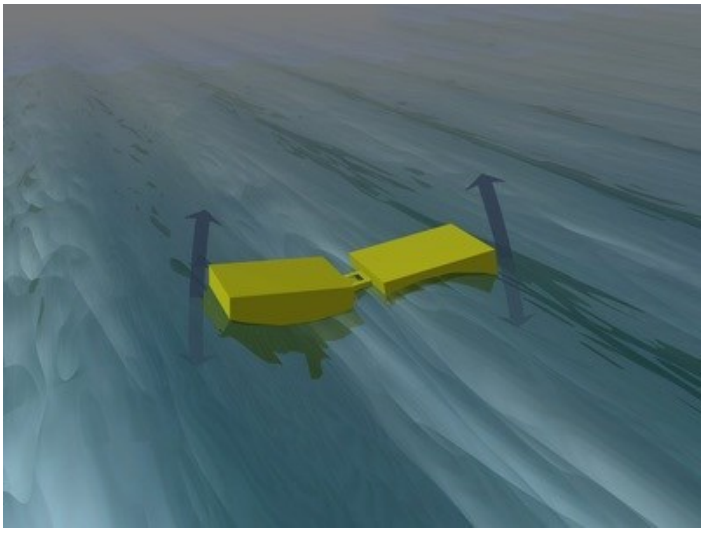

Figure 1.3: Attenuator wave energy converter[10]

Point absorber is a floating object that absorbs energy from all directions by moving around or at the water's surface. It transforms the buoyant top's motion relative to the base into electrical energy. Based on the reactor setup, the power take-ff mechanism will take a variety of shapes[13]. A floating frame with a fixed buoy within a cylinder that rises and falls in response to variations in wave height. The bobbing motion activates a hydraulic system, which transforms the energy into functional electricity [16]. One of the disadvantages of using point absorber is it cannot bear severe storm conditions.

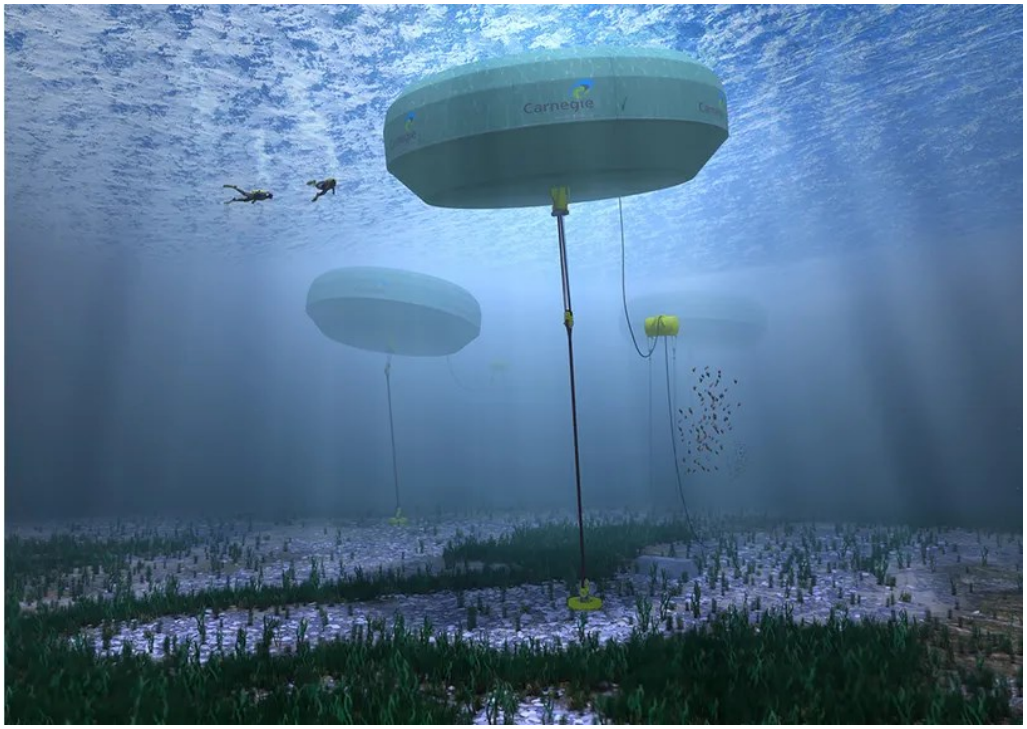

Figure 1.4: Point absorber wave energy converter[12].

The Pelamis is a slack-moored. Offshore wave energy converter made up of a series of semi-submerged cylinders connected by hinged joints[1]. If waves crash into a holding tank, these systems trap the water. The water in then returned to the sea after going

through a low-head turbine that produces electricity[11]. Basically, the amplitude of waves is used by over toppers to fill an attached reservoir to a higher degree than the wave. The excess height is captured in the turbines, which are used to produce electricity through a wire [13]. The Pelamis is worked on by ocean waves that move neighboring cylindrical parts relative to each other through two degrees of freedom joints. The two axes that make up each joint are inclined to the horizontal to allow the power take-off (PTO) mechanism to elicit a net inclined reaction, which resists and reacts against the relative angular motion of the joints. It is this motion which is used to generate electricity [6].

Figure 1.5: Pelamis wave energy converter[14].

Searaser is a wave-driven high-pressure water pump for generating hydro-electric power. The device's oscillatory motion pumps seawater to an elevated tank on min ground, form where the reserved sea-water can be released back downhill through a hydro-electric turbine to produce hydro-electricity, before finally returning back to the sea [6]. The Searaser itself does not generate electricity, but elevates the water (increasing its potential energy) by a combination of buoyancy and gravity forces [16]. The device consists of three main components: Two buoys attached to a piston. It is basically a method to elevate the water mechanically without having to wait for the water cycle.

Figure 1.6: Searaser wave energy converter[15].

1.4 Brief description of the concept of WEC used in this study

1.4.1 Introduction to the *Wave Carpet*

The accretion of mud banks, where the world's second highest dead zone is located, Gulf of Mexico, has formed an area where even the strong waves dampen within a number of wavelengths and there a synthetic seabed carpet supported by generators and springs is expected to extract an analogous amount of energy by responding to the action of overflowing waves and it is in the same way the mud does[17]. Inspired by this theory, in 2014 **Professor Reza Alam** and his students introduced an innovative device that is called ***Wave Carpet***. It is made to float in the water near the shore as a wave energy converter, generating clean, green energy on demand.

1.4.2 Concept and physical model of *Wave Carpet*

They have established the WEC concept[18] that uses a synthetic seabed carpet to transcribe the absorption characteristic of muddy seafloors. The experts used a thin layer of rubber to imitate the influence of a muddy seabed on a series of hydraulic actuators, pipes, and tubes. The pumping of the cylinders generates hydraulic friction and is piped onshore to switch to electricity as the tap drops with the waves up and down. Researchers noted that while rubber is used for experimental research, they look to long-lasting composite materials when a device is installed in the ocean[17]. The seabed carpet is constructed with sets of vertically acting linear springs and generators which is modelled to show action linearly proportional to the vertical speed[18].

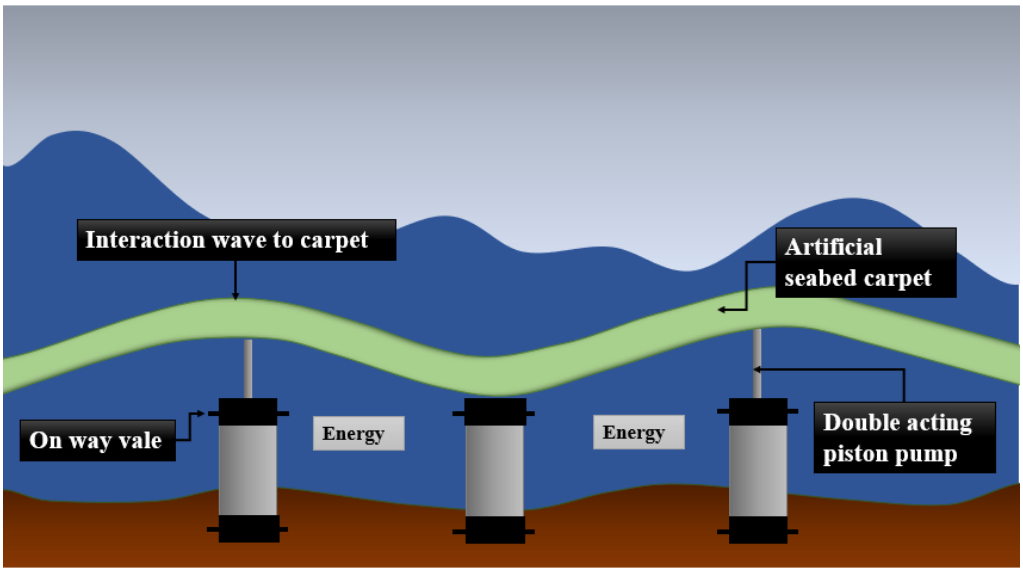

Figure 1.7: Physical model of ***Wave carpet***.

The wave carpet system's coupled governing equation depicts two related ways of propagating wave solution. One is **surface-mode wave**. The higher the frequency, the more energy is extracted by the bottom surface during this wave mode. The other one is **bottom-mode wave** which may provide a clear explanation for the recent observation of strong wave damping of muddy seafloors. Although surface-mode wave damping is

higher for longer waves, bottom-mode damping for shorter waves is higher. In addition, theoretical analysis of nonlinear interactions between surface waves and the rate of energy extraction for steeper surface waves is.

1.4.3 Beneficial aspects of the *Wave Carpet*

The ***Wave carpet*** is capable of supplying power to lots of homes since the coastal areas tend to be well-populated [19] and 40% [16] of the world's population lives within 60 miles of the ocean. The researchers mentioned that every square meter of the carpet generates about 2.5 kilowatts of power out of water near the coast of California which is double the amount of power used by typical American within the same time. Also, for generating the same amount of power, solar panels of size 14 times bigger than this will be needed. However, the ***Wave carpet*** can be planted close to shore. The cables that transfer the power to the grid can be much shorter and thus the power extracted by carpet costs less. So, installation of carpet for WEC is feasible in many ways.

1.5 Objective of this thesis work

By using the novel wave energy conversion device, ***Wave carpet***, the wave energy can be easily utilized and harnessed in efficient way. It is hoped that we will achieve a completely environmentally friendly energy extraction system. The benefit of this research is to contribute to science in the form of an analytical approach. This thesis work has following objectives:

i. To analyze wave energy extraction in different coastal area with varying water depth.
ii. To measure the performance and feasibility of using ***Wave carpet*** in harvesting ocean wave energy by analytical approach.

iii. To estimate and compare incoming wave power to the carpet and energy extraction by the carpet for different country.

iv. To provide input to the development of research for new renewable energy alternatives.

v. To highlight some recommendations for future studies to meet the increasing energy demand in a self-sufficient and long-term manner.

1.6 Organizations of this Thesis

This thesis work comprises of five chapters. Chapter 1 gives a brief overview of the background and concept of this study. Then significance of this research and the objectives of this study are summarized.

A comprehensive literature review is given in the Chapter 2, which categorized into three sections. First section gives a brief overview of the current energy scenario around the world, along with relevant supporting data. In this section, also some ongoing works and research studies in the field of converting wave energy is discussed, including ongoing work conducted by different other authors in that particular field. Other renewable energy sources (other than wave energy), along with their prospects and scopes has been discussed in this section. In the second section, an insight into the analysis of wave energy converters is given briefly. Section three is all about the ***Wave carpet*** which gives a brief summary, summing up all the information and key points discussed throughout the literature review.

Then Chapter 3 describes the methodology of the study. Some underlying assumptions that have been adopted for the simplification of our calculation, are also stated there.

After that Chapter 4 describes the findings and end results of the overall performance evaluation.

The conclusions and summary of the contributions are presented in chapter 5. In addition, some directions for future work related to this study are also presented. Finally, Chapter 6 lists the literature cited in this work.

Chapter 2 Literature Review

At present, among many more renewable energy sources, oceanic wave energy is the cost friendly and most efficient energy source which could be a good competitive source to mitigate the increasing needs for cleaner and greener energy.

2.1 Current Energy Scenario

During the 1970s oil crisis, several disappointing experiments dashed high expectations for wave power[20], interest dramatically has been increased with the introduction of several new technologies which can improve the efficiency and viability of wave energy. With recent advancements, companies are investing in wave energy devices all over the world.

Limpet 500, the world's first commercial wave plant, was installed on the Scottish island of Islay in 2000 and has been supplying electricity to the UK grid since late November 2000[21]. The Limpet 500 is a Wavegen 0.5 MW plant with an oscillating water column design that can be installed on exposed shores[20]. Wavegen has also developed OSPREY 2000, a near-shore device (Ocean Swell Powered Renewable Energy), a 2 MW station for 15 m deep water up to 1 km from the shore, and the WOSP 3500, a combined OSPREY and offshore windmill unit, rated at a total of 3.5 MW (2 MW OSPREY plus 1.5 MW wind)[22].

Also, on the island of Islay, Ocean Power Delivery Ltd. of Edinburgh, Scotland is bringing in a small wave power system off the coast that can power up to 200 homes[20]. In 2002, the installation should be completed. The plant can generate 2.5 million kW hours of electricity each year. With support from the Scottish Renewable Obligation of

1999, OPDL eventually plans to install up to 900 devices, with a total capacity of 700 MW, producing more than 2.5 billion kW h/yr. Since August 1990, the Monitor, a Demi-Tek hybrid device that incorporates tidal, wave, and wind control, has been running just off the coast of Asbury Park, New Jersey. The Monitor generates enough energy to power the city's boardwalk and convention center. In addition, the Control was deployed to assist in the mitigation of wave activity and erosion security on beaches. Cables similar to those used for underwater oil exploration anchor it to the ocean floor, and an undersea cable carries power to land[23].

2.1.1 Renewable Energy Resources and Their Prospects

From 2011 to 2030, global energy demand will rise by 36%, at an average growth rate of 1.6 percent, with fossil fuels accounting for 88 percent of the total[1]. Sources like wind, solar, geothermal and biomass are studied in this section.

2.1.1.1 Biomass

Rice husk, grain residue, jute stick, timber, animal waste, municipal waste and so on are all forms of biomass. It is the world's fourth-largest energy sources. Biomass accounts for 8.5 percent of global final energy consumption at the moment[24]. It has the potential to boost the environment quality of the atmosphere by lowering pollution and as a promising source of energy production. In terms of demand, biomass energy will account for 50% of global energy consumption by 2050[25].

2.1.1.2 Solar Energy

Solar energy is today considered to be one of the most promising renewable energy sources worldwide. It has the highest energy potential, as compared to other renewable

resources. Solar energy is used in a range of uses, including lighting, heating, and , most notably, power generation.

2.1.1.3 Wind Energy

Wind energy is now one of the most growing clean energy markets[26]. In Germany, wind energy accounts for 38.1 percent of overall power production. However, Commercial wind turbine power generation necessitates a through techno-economic study, which is not readily accessible[1].

2.2 Works on Wave Energy Converter

We can find many reviews of wave energy converter (WEC) concepts from a number of sources. S.H. Salter[27]explained about a different concept of wave energy converter where hydrogen has been used as an energy source. T W Thorpe has showed in his report[28] that many wave energy systems are being studied but most are only in the research and development stage, with only a limited number of devices having been performed on a wide scale and deployed in the oceans. One facility that is currently providing electricity for the National Grid is the LIMPET shoreline oscillating water column (OWC), which was constructed in Islay, Scotland, in 2000[29]. Another commercial wave power plant began service in Northern Portugal in September 2008. Pelamis wave (formally OPD) in Scotland designed the Pelamis power generation unit for it. L. Margheritini addressed an overtopping style wave energy converter (WEC). Based on the wave height, the overtopping water of incoming waves was deposited in various basins[1].

2.3 Summary

Wave carpets are designed to harness energy from wave energy from different coastal areas around the world where the wave potential is comparatively higher. In this regard, ***Wave carpet*** a noble wave energy converter invented by Reza Alam has great potential and flexibility to harness energy from the ocean. If we can utilize the energy extracted from ***Wave carpet*** in a good way, we can enrich preservation of the natural environment and help sustain the local population by fulfilling their energy demands.

Chapter 3 Methodology

3.1 Introduction

Professor Reza Alam all together with his PhD students in Mechanical Engineering Department (University of California, Berkeley) are experimenting a prototype of a device, see Figure 3.1, which can provide clean drinking water for coastal communities around the world and also produce electricity, is called a Wave Energy Converter also known as ***Wave Carpet***. This device attempts to harness the predictable wave power to obtain utilizable energy. The carpets motion produces hydraulic pressure energy when the waves pass through. This usable energy can be used to turn turbines and generate electricity and also be able to produce fresh water by reverse osmosis. The fresh water is obtained when the pressurized salt water is pushed through the membranes which extract the salt. The researchers choose regions which do not have enough oxygen to support marine life in order to plant ***wave carpets*** and this system avoids negative impacts on marine ecosystem. Therefore, 15% of the global energy demand can be achieved by this technology [1].

Taking inspiration from the nature, for example, if some amount of substantial energy can be taken out of incident surface gravity waves by muddy seafloor, an artificial carpet introduced to the seabed can also be responded to the action of the overpassing waves in the similar manner as the response of a muddy seafloor, must be able to extract the same amount of energy which is introduced by Professor Alam [30]. Similarly, a synthetic seabed carpet[17], which is supported by springs and generators, see Figure 3.1, is expected to extract some substantial energy by responding to the action of the overpassing waves in the same way the muddy seafloor does.

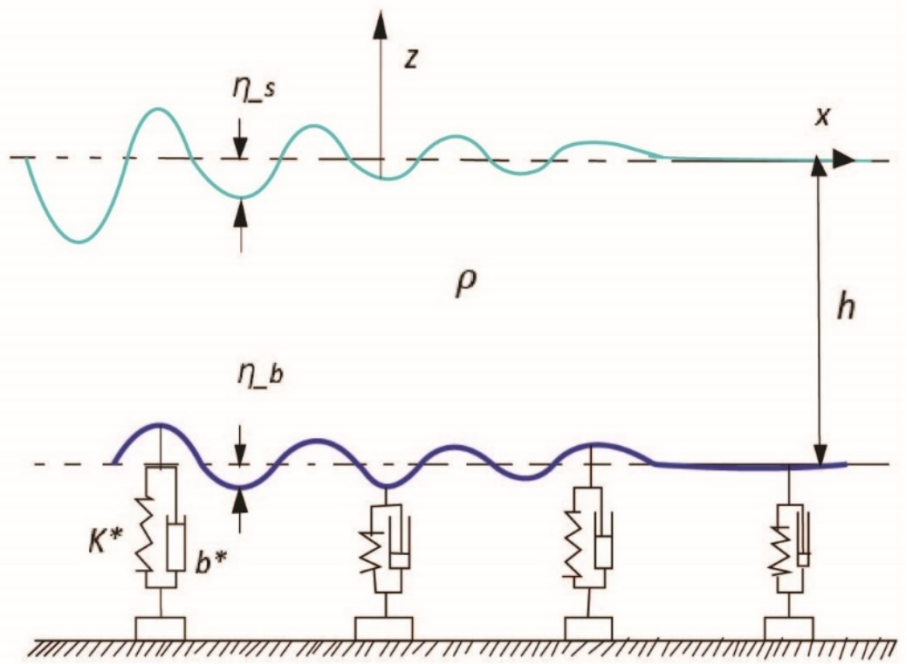

Figure 3.1: A ***Wave Carpet*** consisting of a synthetic viscoelastic carpet with linear springs (k^*which is stiffness coefficient that provides restoring force) and double acting dampers (b^*which is damping coefficient that extract energy)

3.2 Components of *Wave carpet*

The ***Wave Carpet*** is consisted with four basic components which is shown schematically in Figure 3.2. The four components are operated together sequentially by following some specifications. The absorbed energy of the influencing waves is bundled to the Absorber Carpet, to the Connection, which transmitted the energy to the hydraulic Power Take Off (PTO) units. PTO units converted the kinetic energy into a mechanically sustainable energy, the Mooring is connected to the bottom of the PTO units with the bottom side of the tank[17].

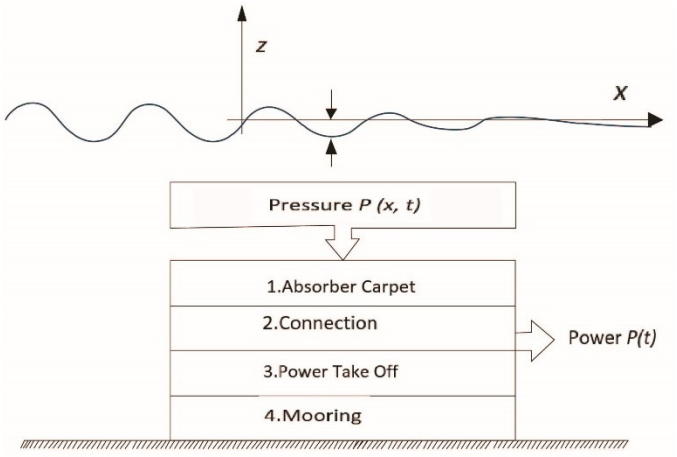

Figure 3.2: Components of ***Wave Carpet***[17]

i. **Absorber Carpet:** In order to accomplish the ***Wave Carpet*** specifications[17] a material with anisotropic specification is needed.

ii. **Connection:** Below the Carpet, there is a direct physical connection with a aluminum bar whereas the PTO is linked to the shaft[17].

iii. **Power Take Off System (PTO):** Operating in a double acting manner, the entire PTO unit dampens the Absorber Carpet in dual upward and downward motions[17].

iv. **Mooring:** The PTO units are connected to the bottom of the tank with a hinge[17] by Mooring that permits the PTO units to revolve around y-axis. Since the motion of overpassing waves is acquired by the Carpet, the upper part of the piston shafts will be replaced in z-axis and x-axis direction[17]. Therefore, the potential of revolving around the y-axis is required by the PTO units.

3.3 Assumptions

- *Deep water:* The common state in the seas and ocean deep-water along with a water depth larger than half the wavelength[31]. Longer-period waves circulate faster and conveyance their wave energy faster in deep water. The phase velocity is double of the deep-water group velocity[31]. That's the reason, we consider deep-water depth for calculation purpose.

  Where, $\tanh \mu = 1$ Which is $(\tanh \mu \frac{2\pi h}{L} = 1)$

- Linear solutions have been applied to the governing equations.
- The area of the ***wave carpet*** is assumed to be 1 m^2 for this study purpose.

3.4 Reasons of selection the coastal areas of the country

Ò **Australia:** In the 19th century within areas of heavy rainfall and elevation in Australia (i.g. New South Wales and Tasmania), hydropower was developed[32]. So far, hydropower remakes the largest contribution to "Australian renewable energy generation, accounting for 40% in 2016-2017" [32]. Moreover, , "it is estimated that wave energy alone could contribute up to 11% of Australian's total energy needs by 2050"[32]. By using ***Wave Carpet***, we can extract sufficient amount of wave energy which can be the solution of more dependency of renewable energy sources, especially ocean energy.

Ò **Belgium:** The wave energy translation has not undergone substantial development in Belgium due to political reasons, mainly focusing on other energy sources[33] and also lack of feasible resources. Belgium also has a quite limited length of coastline, high offshore traffic density and shallow coastal water[33]. All these issues oppose noteworthy interest in wave energy

development in this particular place. Despite of these limitations, ***Wave Carpet*** technology can be placed and extract significant wave energy.

- **China:** In China, the insufficient amount of fossil fuels and low energy efficiency, ocean energy becomes the most observable form of energy[34]. The extraction of wave energy can be a solution to the vast power requirements of a country like China having huge coastline of more than 18000km and a sea area of more than 34,00,000 km^2 with plentiful ocean energy resources[34]. ***Wave Carpet*** can be planted in these coastal areas and extracted sufficient amount of wave energy.
- **India:** India has been looking ahead to discover green and renewable sources of energy in the form of wave energy, by reason of having the lengthiest coastline of about 7500 km[35]. In fact, about 35% of India's population survives within 100 km range from the coastline[35].
- **Italy:** Italy has a long coastline in relation to its land area and would approach suitable for application of ocean energy[33]. "In general, the wave energy annual average is less than 5KW/m"[33]. Therefore, some explicit locations, such as Sicily or Sardinia, has the higher mean wave energy, up to approximately 10 KW/m[33].

3.5 Calculation of dimensionless parameters of the *Wave carpet*

3.5.1 Equations of velocity potential (ϕ)

It is described that the behaviour of an actuated seafloor mounted carpet for a high-performance wave energy extraction [5], [6] where a homogeneous inviscid incompressible fluid with irrotational motion is considered. Therefore, z=-h references the mean depth of the bottom (which is viscoelastic), see Figure3. The equations [3], [6] of the velocity potential ϕ ignoring the surface tension, and the surface and bottom elevations η_s and η_b are described below:

$$\nabla 2\varphi = 0, -h + \eta_b < z < \eta_s \tag{1}$$

$$\eta_{s,t} + \eta_{s,x}\varphi_x = \varphi_z, z = \eta_s \tag{2}$$

$$\varphi_t + 1/2(\varphi_x^2 + \varphi_z^2) + g\eta_s = 0, \qquad z = \eta_s \tag{3}$$

$$\eta_{b,t} + \eta_{b,x}\varphi_x = \varphi_z\,, \;\; z = -h + \eta_b \tag{4}$$

$$\varphi_t + \frac{1}{2(\varphi_x^2 + \varphi_z^2)} + g\eta_b + \frac{P_b}{\rho} = 0, \qquad z = -h + \eta_b \tag{5}$$

$$b^*\eta_{b,t} + K^*\eta_b + P_b = 0, \; z = -h + \eta_b \tag{6}$$

Where the stiffness coefficient of the viscoelastic bottom per unit area is K^*, the viscous damping is b^*, the pressure on the seabed is P_b, the density of the fluid is ρ, the gravity acceleration is g. The linearized form of the above governing equations states a propagating wave in the form of [17], [18]

$$\eta_s = a_s e^{i(kx-\omega t)} \tag{7}$$

$$\eta_b = a_b e^{i(kx-\omega t)} \tag{8}$$

$$\varphi = (Ae^{kz} + Be^{-kz})e^{i(kx-\omega t)} \tag{9}$$

Where,

$$a_b = a_s \cosh k \left(1 - \frac{gh\, tanh\, kh}{\omega^2}\right) \tag{10}$$

$$A = -ia_s \frac{\omega^2 + gk}{2k\omega},\ B = ia_s \frac{\omega^2 + gk}{2k\omega} \tag{11}$$

Where a_s is the surface amplitude and a_b is the bottom amplitude.

3.5.2 Dispersion relationship

The dispersion relation can be read as dimensionless form[18] that is

$$\gamma\Omega^4 \tanh\mu + i\mu\gamma\zeta\Omega^3 - \mu\Omega^2 - i\mu^2\gamma\zeta\Omega \tanh\mu + \mu^2(1-\gamma)\tanh\mu = 0 \tag{12}$$

Where, $k = \frac{2\pi}{L}$ and $\mu = kh$. We consider deep water for classification of ocean depth[36]

so $\tanh\mu = 1$;$(tanh\frac{2\pi h}{L} = 1)$for applicable in Equation 12.

In this case, damping[18] is non-zero $(\zeta > 0)$ and the deep water limit is μ>>1, the dispersion relation Equation 12 is simplified to

$$(\Omega^2 - \mu)[\,\gamma\Omega^2 + i\mu\gamma\zeta\ \Omega - \ \mu(1-\gamma)] = 0 \tag{13}$$

Roots of the bottom mode bracket of Equation (13) show a bifurcation at a critical (dimensionless) depth. The behavior [18] of the bottom mode waves is much complex.

$$\mu_{cr} = \frac{4(1-\gamma)}{\zeta^2\gamma} \tag{14}$$

The dimensionless variables are[17], [18], [30]

$$\Omega = \omega\sqrt{\frac{h}{g}} \ , \quad \zeta=\frac{b*}{\rho\sqrt{gh}} \ , \quad \gamma = \frac{\rho g}{k*} \ , \ and \ \mu = kh \tag{15}$$

Where the shallowness is μ, dimensionless restoring force is γ (the ratio of hydrostatic restoring coefficient to the bottom elasticity), ζ represents the dimensionless damping ratio and Ω expresses the dimensionless frequency.

3.5.3 Undamped solution of dispersion relation equation

Moreover, considering necessary conditions and for any specific μ, Equation 12 with ζ=0 achieves two real solutions[18] for Ω. The simplified forms[18] of the two undamped solutions of Equation12) in the limit of deep water (where μ>>1) are

$$\Omega_s = \sqrt{\mu} \tag{16}$$

$$\Omega_b = \sqrt{\frac{\mu(1-\gamma)}{\gamma}} \tag{17}$$

Where Ω_s references as surface dimensionless frequency and Ω_b references as bottom dimensionless frequency.

3.5.4 Calculation of Wave Length

We can get the wave length by the following formula[37],

$$L = \frac{gT^2}{2\pi} tanh\left(\frac{2\pi d}{L}\right) \tag{18}$$

Eckart (1952) gives an approximate explicit expression for Equation16, which is correct to within about 5 percent[37].

This expression is given by

$$L = \frac{gT^2}{2\pi}\sqrt{tanh\left(\frac{4\pi^2 d}{T^2 g}\right)} \tag{19}$$

3.5.5 Plot of undamped solutions

Now, Equation14 expresses the dispersion relation of deep-water waves and it is unaffected by the bottom elasticity. The Equation 14 which is the surface mode in the limit of deep-water results in $a_b \ll a_s$ which means the carpet amplitude is much smaller than the surface amplitude and hence is of less physical significance[18].

Therefore, undamped solutions of Equation 12 are plotted in below Figures for three values of γ = 0.1, 0.5, 0.9.

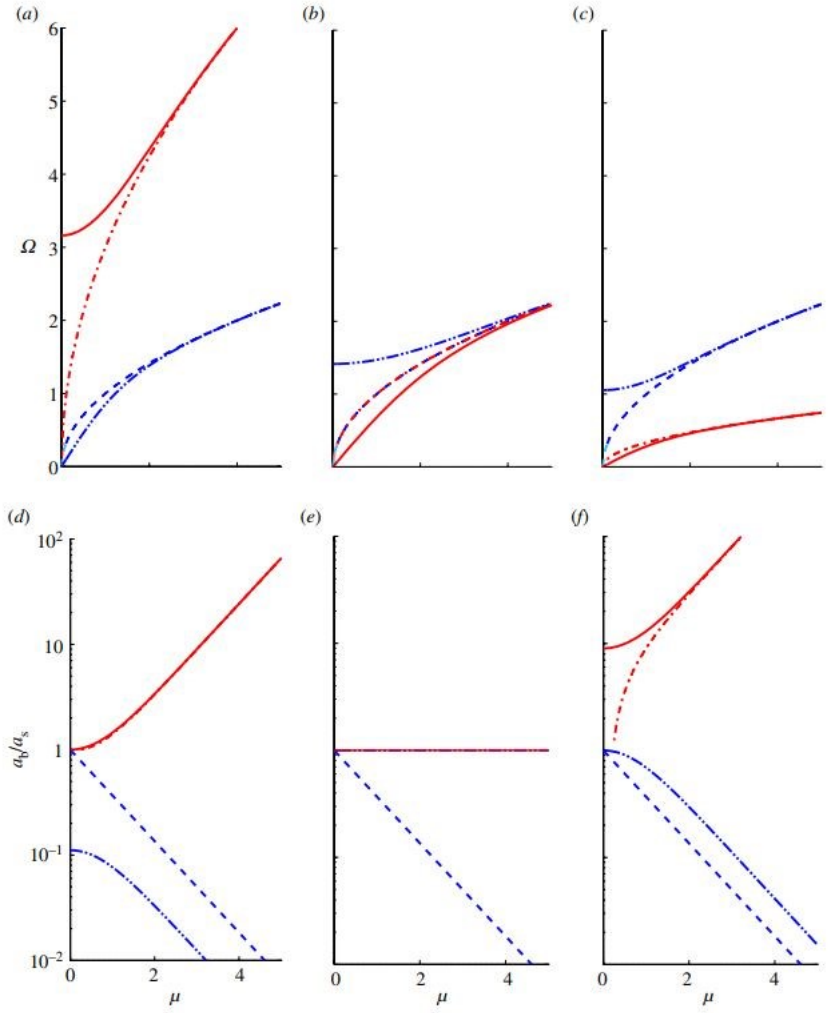

Figure 3.3: A group of graphs shows the Equation 12 with ζ=0 and Equation 10.

From the above Figure 3.3, a group of graphs shows the Equation 12 with ζ=0 and Equation 10. Dashed dotted-dotted-line of (a-c) represents surface mode and solid line of (a-c) represents bottom mode solutions to the Equation 12 for γ = 0.1, 0.5, 0.9 respectively. The dashed line for Equation 16 and dashed-dotted line for Equation 17 are also plotted for comparison. The deep-water dispersion relation of Equation 16 when $\gamma = \gamma_{cr}$ = 0.5 tends to follow asymptotical curve shapes. The Equation 10 of the ratio of bottom elevation amplitude to surface elevation amplitude for γ = 0.1, 0.5, 0.9 is also shown as (d-f) figures [18].

it can be said that for a surface mode solution $a_s > a_b$, and for a bottom mode solution $a_s < a_b$, expect for $\gamma = \gamma_{cr} = 0.5$, for which as μ increases[18], the surface and bottom mode solutions asymptotically tend to each other and towards the deep-water dispersion relation in Equation 16, which is shown in Figure 3.3 (b).

For a sub-critical $0 < \gamma_{sub} < \gamma_{cr}$, any given wavenumber[18] is associated with one surface mode wave and one bottom mode wave, with the frequency of the bottom mode wave being much higher than that of the surface mode, see Figure 3.4 (a). The inverse case holds for the supercritical $\gamma_{cr} < \gamma_{sub} < 1$ where the frequency of a surface mode wave is limited by the $\Omega_{min} = \frac{1}{\sqrt{\gamma_{sub}}}$ [18].

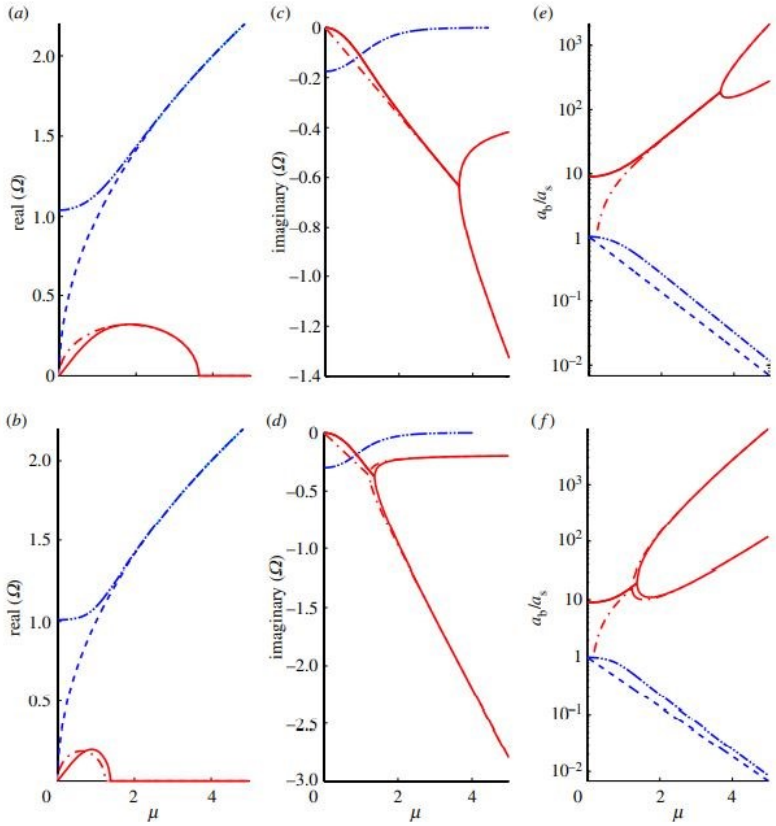

Figure 3.4: A group of graphs shows real branched of the solution $\Omega(\mu)$ and imaginary branched of the solution $\Omega(\mu)$ to the Equation 12 for γ = 0.9 and for ζ = 0.35 and for ζ =0.60.

In this above case, see Figure 3.4, A group of graphs shows real branched of the solution $\Omega(\mu)$ in (a, b) and imaginary branched of the solution $\Omega(\mu)$ to the Equation 12 for γ = 0.9 and for ζ = 0.35 in (a, c), for ζ =0.60 in (b, d). The ratio of the bottom amplitude to the surface amplitude is also plotted in (e, f). Dashed-dotted-dotted line of surface mode and solid line of bottom mode are also associated with the plotted graphs. The division of the graphs into two branches at $\mu_{cr} = 3.62$ and μ_{cr}=1.23 (in Equation 14). The branches of deep-water asymptotes in Equation 13 are plotted in dashed and dashed-dotted lines respectively[18]. The ratio of the bottom amplitude to the surface amplitude is also plotted in (e, f). Dashed-dotted-dotted line of surface mode and solid line of bottom mode are also associated with the plotted graphs. The division of the graphs into two branches at $\mu_{cr} = 3.62$ and μ_{cr}=1.23 (in Equation 14). The branches of deep-water asymptotes in Equation 13 are plotted in dashed and dashed-dotted lines respectively[18]. depending on the value of Ω_b [18],shorter waves may be damped much faster or asymptotically approach a wavelength which is not dependent on decay rate.

On the other hand very short waves are still damped, and are stronger than the rate of decay of the longest surface waves[18]. Here we approach at the critical shallowness, $\mu = \mu_{cr}$ and there is only one damping rate[18].

In conclusion we can say that the coupled system of gravity waves and our carpet acknowledges the surface mode and the bottom mode of the wave. The bottom mode shorter waves are damped faster whereas for a rate of decay of a surface mode wave is higher for longer waves, this is a major difference between the two mode[30]. The concept presented here can, essentially, incorporate any mud model and its performance under different models may worth further inquiry[30]. Therefore, if frequency

dependent damping and stiffness coefficients are combined the performance may be substantially increased[30].

3.6 Calculation of Energy Extraction by *Wave carpet*

3.6.1 Calculation of total energy

For a undamped system the energy stored in the carpet per unit area is described as,[17]

$$E_{tot} = E_{Kin} + E_{pot} = \frac{1}{2}\rho g a_s^2 D \tag{20}$$

With

$$E_{Kin} = \frac{1}{4}\rho g a_s^2 [\frac{\sinh 2kh}{2}\left(\frac{\omega^2}{gk} + \frac{gk}{\omega^2}\right) - 2sinh^{\,2}\, kh] \tag{21}$$

$$E_{pot} = \frac{1}{4}\rho g({a_s}^2 - {a_b}^2) + k^* {a_b}^2 \tag{22}$$

$$E_{tot} = \frac{1}{2}\rho g a_s^2 \left[\frac{\sinh 2kh}{2}\left(\frac{\omega^2}{gk} + \frac{gk}{\omega^2}\right) - 2sinh^2 kh + \rho g({a_s}^2 - {a_b}^2) + k^* {a_b}^2\ \right] \tag{23}$$

3.6.2 Calculation of dimensionless constant for energy extraction

The solution of Equation12 gains an imaginary part $\omega = \omega r + i\omega i$

The dimensionless constant is written as D_d if damping is present[17]

$$D_d = \frac{1}{2}\left[\frac{sinh2\mu}{2}\left(\frac{{\Omega_r}^2}{\mu} + \frac{\mu}{{\Omega_r}^2}\right) - 2(sinh\,\mu)^2\right] + \frac{1-\alpha}{2} + \frac{\alpha}{2\gamma} \tag{24}$$

Here, Ω_r is the real part of the dimensionless Ω and the dimensionless amplitude ratio of the bottom to surface[17]

$$\alpha = \frac{a_s^2}{a_b^2} = \cosh^2\mu(1 - \frac{\mu \tanh \mu}{\Omega^2}) \tag{25}$$

with $a_s(t) = a_{s0}\, e^{\omega i t}$.

3.6.3 Calculation of energy in dimensionless form

Hence the energy in the dimensionless form can be written as[17]

$$\epsilon = \frac{1}{2} e^{(2\Omega\_i\,\tau)} Db \tag{26}$$

Where, $\tau = T\sqrt{\frac{g}{h}}$

For one period of time the amount of energy, the carpet extracts[17] is

$$E_c = \frac{1}{2}\rho\ g\ a_{s0}^2\ \epsilon\ Ac \tag{27}$$

Where A_c expresses the area of the carpet.

3.7 Incoming Power of Wave to the *Wave carpet*

The wave power is calculated as[17]

$$P_{wave} = \frac{1}{2}\rho g C_g a^2 W \tag{28}$$

Where W represents carpet width, g represents gravity acceleration, ρ expresses the density (1030 kgm^3), group velocity[17] of the wave is

$$C_g = \frac{1}{2}(1 + \frac{2kh}{\sinh 2kh})Lf \tag{29}$$

3.7.1 Efficiency of *Wave Carpet*

Now the Wave-Carpet efficiency[17] stands for

$$Efficiency = (E_c)/P_{wave} \tag{30}$$

To validate the accuracy and wave power extraction from the ***Wave Carpet***, a fully nonlinear solution to the governing Equation (1-6) achieved by Newton's iterative

method[30] should be used. For estimating the amount of wave-energy the Wave-Carpet can absorb or utilize, it was implemented in the selected places by mathematical study. But in this paper, we use linear solutions rather than nonlinear solution.

Chapter 4 Results and Major Findings

4.1 Wave Data Characteristics

We have implemented the formulas in some selected coastal regions in order to extract wave energy from ***Wave Carpet***. Following to the methodology described in section 3.3 and 3.4 incoming wave power to ***Wave Carpet*** and energy extraction by ***Wave Carpet*** is calculated. The results are arranged in Table 4.1. In this work we collected the data of Australia because, 'it is estimated that wave energy alone could contribute up to 11% of Australian's total energy needs by 2050'[32]. From European continent we collected the data of Belgium and Italy because those data are available for the validation of our calculation. Among selected European Continent, Belgium shows better performance of using the above section equations (section 3.3 and 3.4) than Italy. Moreover, from the Asian continent we collected wave data from China, India since they were available and we used them to verifying above equations. Among the selected Asian continent, China shows better performance in incoming power to the ***Wave Carpet*** and energy extraction by the ***Wave Carpet***, which we will see in the following results.

A set of nine wave profiles of South coast of Tasmania, Australia[38], four set of wave profiles of Belgium coastal area of the North Sea[39], also a set of eight profiles of Adjacent seas which are including the Bohai Sea, yellow sea, east China Sea, as well as the Northern South China Sea[40]–[42], beside these a set of seven wave profiles of Shelf seas of India[43], [44], also a set of nine wave profiles of Pantelleria Island (Sicily), Italy[45], have been chosen to execute the analytical calculations. In Table 4.1,

the wave period *T*, the significant wave height *H*, the water depth h, the incoming wave power to the ***Wave Carpet*** P_{wave} and energy extraction by the Wave Carpet (when γ=0.9, ζ=0.35) are reported together.

Table 4.1: Incoming Power(kW) to the *Wave Carpet* and energy extraction (when γ=0.9, ζ=0.35) (kW) by the Wave carpet (different geological locations of coastal region).

Country	**Location & Continent**	**Country Latitude & Longitude**	***h*** **(m)**	***H*** **(m)**	***a*** **(m)**	***T*****(s)**	**Incoming Wave Power (kW)**	**Energy extraction (kW) γ=0.9, ζ=0.35**
Australia [38]	South coast of Tasmania (Oceania)	-27 144	50	0.75 1.25 1.75 2.50 3.25 4.25 5.25 5.75 6.25	0.38 0.63 0.88 1.25 1.63 2.13 2.63 2.88 3.13	4.00 5.00 6.00 7.00 8.00 9.00 10.00 11.00 12.00	2.21 7.65 17.80 41.80 79.98 154.24 265.37 357.72 471.26	0.36 1.01 1.99 4.04 6.47 9.67 11.66 9.80 7.46
Belgium [39]	Belgian coastal area of the North Sea(Europe)	50.85 4.35	22	0.25 1.25 2.50 3.75	0.13 0.63 1.25 1.88	3.00 4.00 5.00 6.00	0.18 6.05 29.67 80.09	0.04 1.01 4.00 7.94
China [41][42]	Adjacent seas (Asia)	39.92 116.38	50	3.10 3.25 2.65 2.60 2.45 2.90 3.40 3.35	1.40 1.63 1.33 1.30 1.23 1.45 1.70 1.68	7.70 7.60 6.90 7.05 7.55 7.93 8.35 8.40	70.17 76.19 46.36 45.51 43.03 63.15 91.30 89.17	6.03 6.68 4.55 4.36 3.79 5.17 6.81 6.56
India [43][44]	Shelf seas of India (Asia)	28.61 77.21	71	1.30 1.40 1.13 1.50 0.90 0.80 1.00	0.65 0.70 0.57 0.75 0.45 0.40 0.50	7.63 7.46 7.90 7.80 5.67 5.90 6.80	12.42 14.11 9.68 16.87 4.50 3.69 6.61	1.09 1.27 0.82 1.46 0.52 0.41 0.65
Italy [45]	Pantelleria Island, Sicily (Europe)	41.9 12.48	32	1.18 1.97 0.67 0.68 1.36 2.20 1.45 1.99 0.69	0.59 0.99 0.34 0.34 0.68 1.10 0.73 0.99 0.35	5.31 6.44 7.38 6.54 6.83 8.09 7.77 7.27 5.36	7.10 23.65 3.15 2.86 11.95 37.78 15.64 27.34 2.44	0.91 2.36 0.17 0.26 1.02 1.76 0.81 2.00 0.31

4.2 Incoming Wave Power to the *Wave carpet*

A large scale WEC, ***Wave Carpet*** allocated in the ocean can be operated to generate power and to cancel out waves[17]. A visco-elastic mud mechanism is also similar to the WEC by damping the energy of overpassing surface waves,[30] in the case of carpeting the near-shore seafloor by an elastic thin material connected to generators (i.e. dampers) can absorb a high fraction of surface wave energy. Therefore, a substantial energy can be taken out of incident surface gravity waves by the muddy floor, as long as an artificial ***Wave Carpet***[30] installed on the seabed that responds to the influence of the overpassing waves in the same way as the response of a muddy floor must be able to extract the same aggregate of energy which is subjected to this paper through analytical expressions of power extraction by the ***Wave Carpet***. See Figure 4.11, a geographical plot is given where we can visualize the incoming wave power to the ***Wave Carpet*** of different coastal regions. From this graph, South coast of Tasmania of Australia can afford the higher amount of incoming wave power (471261.77 Watt) to the ***Wave Carpet*** than any other selected coaster regions. The high pressure water generated by the wave power extraction [17] can be used: 1) to generate electricity by running a hydraulic turbine; 2) to produce fresh water by supplying a reverse osmosis process; 3) and to allocate fresh water.

4.2.1 Effect of incoming wave power on Wave period

Relation of incoming wave power with wave period taking wave height constant can be clarified by plotting scatter graphs of different country.

Table 4.2: Effect of incoming wave power on wave period while keeping the wave height constant.

Country	***h*(m)**	***H*(m)**	***T*(s)**	**Incoming Wave Power (Watt)**
Australia *South coast of Tasmania (Oceania)*[38]	50	1.25	4.00 5.00 6.00 7.00 8.00 9.00 10.00 11.00 12.00	6152.24 7650.39 9084.07 10451.96 11832.47 13343.30 15043.74 16905.62 18850.47
Belgium *Belgian coastal area of the North Sea(Europe)*[39]	22	1.25	3 4 5 6	4604.45 6152.24 7419.25 8899.31
China *Adjacent seas which includes the Bohai Sea, Yellow Sea, East China Sea, as well as the Northern South China sea (Asia)* [41][42]	50	3.25	7.70 7.60 6.90 7.05 7.55 7.93 8.35 8.40	77128.92 76190.79 69739.89 71113.11 75724.01 79313.84 83428.21 83930.59
India *Shelf seas of Indian (Asia)*[43][44]	71	1.40	7.63 7.46 7.90 7.80 5.67 5.90 6.80	14410.89 14118.06 14872.81 14702.11 10901.32 11328.27 12961.59
Italy *Pantelleria Island, Sicily* [45]	32	1.97	5.31 6.44 7.38 6.54 6.83 8.09 7.77 7.27 5.36	19791.91 23653.61 27240.34 24012.36 25080.96 30294.79 28882.74 26793.74 19960.57

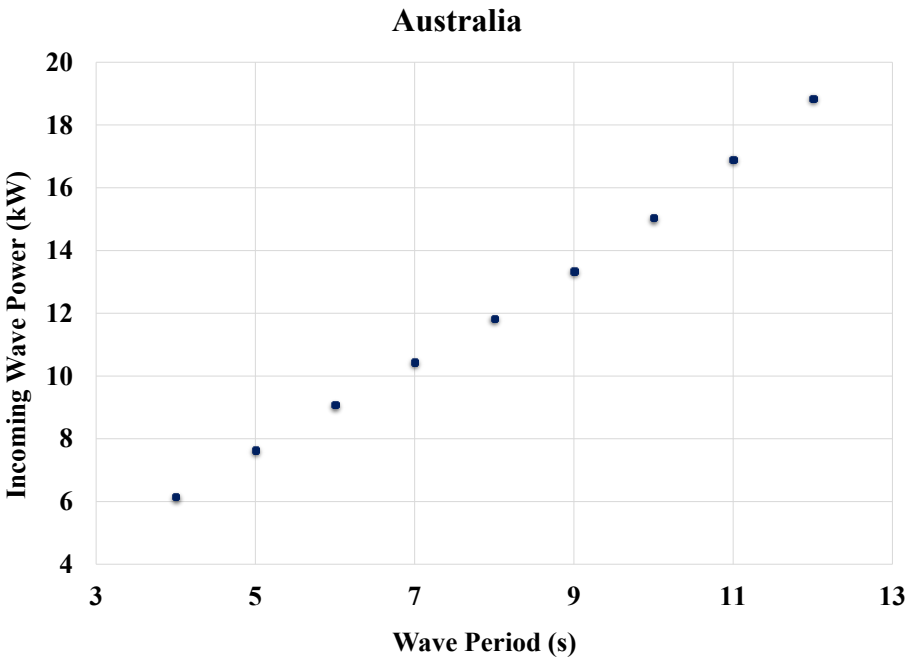

Figure 4.1: Effect of incoming wave power on wave period while keeping the wave height constant (**Australia** South coast of Tasmania).

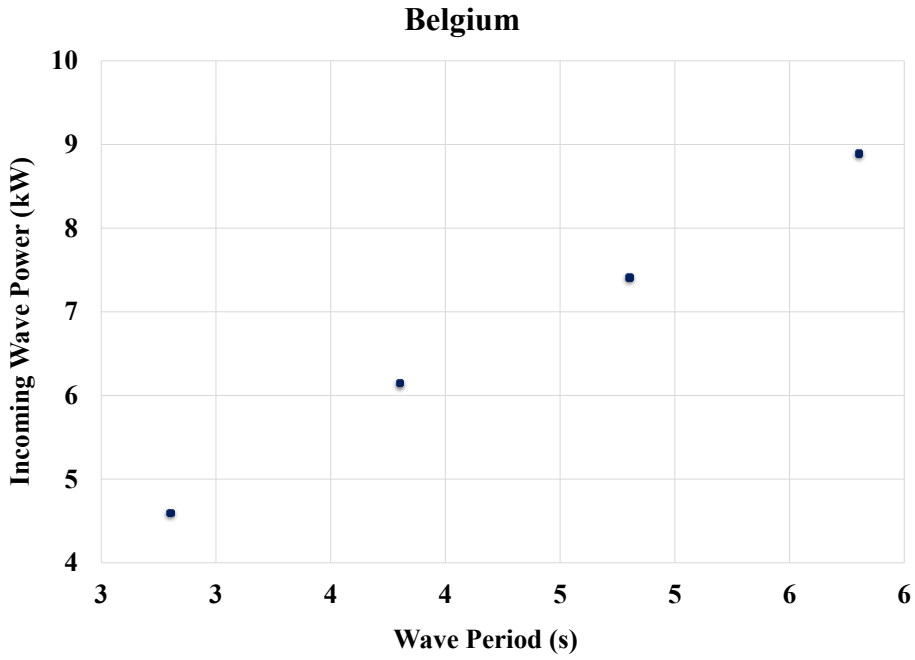

Figure 4.2: Effect of incoming wave power on wave period while keeping the wave height constant (**Belgium** Belgian coastal area of the North Sea).

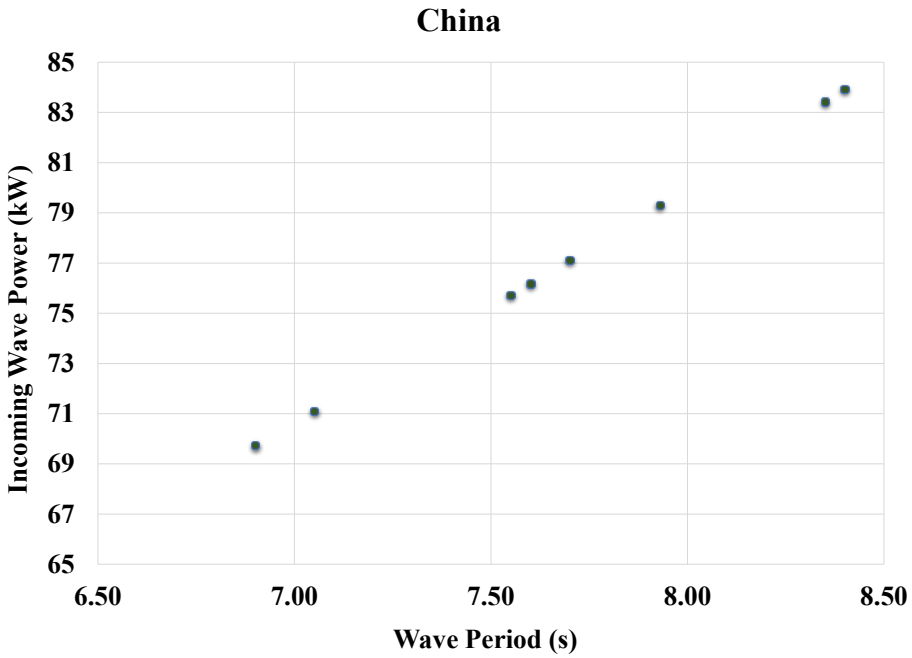

Figure 4.3: Effect of incoming wave power on wave period while keeping the wave height constant (**China** Adjacent seas)

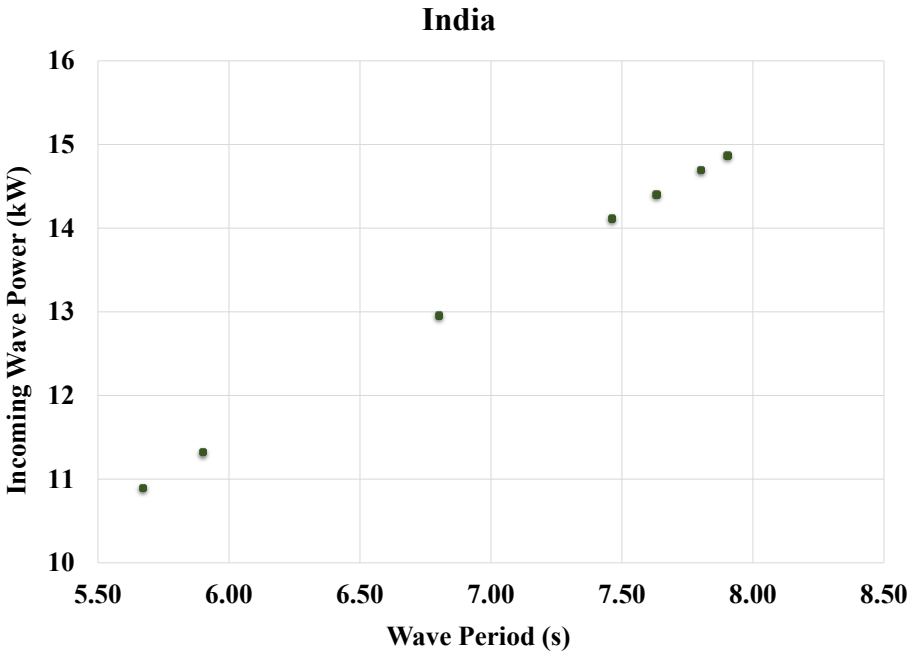

Figure 4.4: Effect of incoming wave power on wave period while keeping the wave height constant (**India** Shelf seas of India).

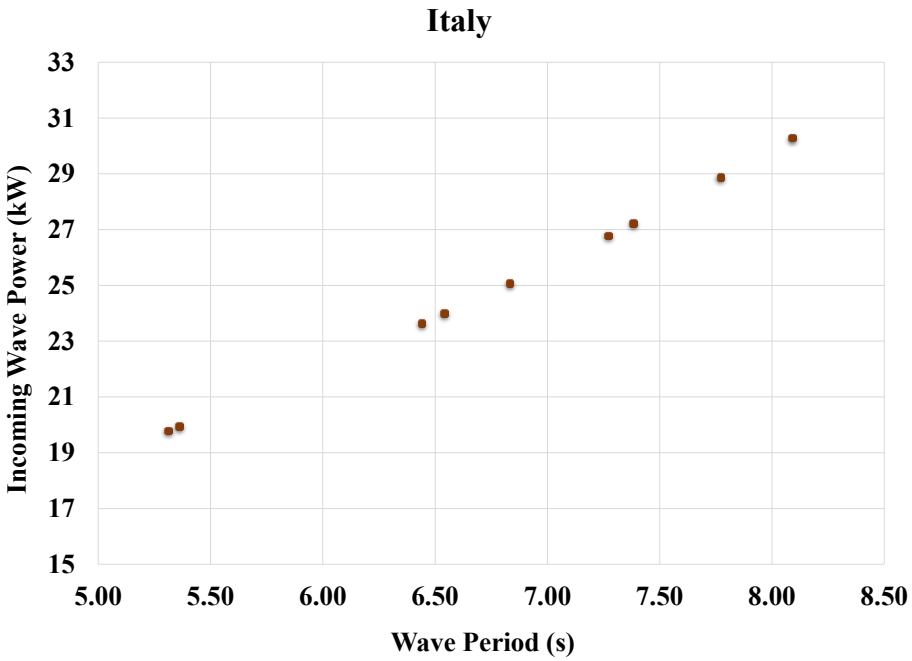

Figure 4.5: Effect of incoming wave power on wave period while keeping the wave height constant (**Italy** Pantelleria Island, Sicily).

In the above Figure 4.1-Figure 4.5, the graphs were plotted with the help of Equation 28 and 29 which shows a linear relationship with the two parameters in each of them. The graphs were plotted by using the data from Table 4.2. Increasing the wave period may increase the incoming wave power to the ***Wave Carpet***. The higher the amount of incoming wave power the ***Wave Carpet*** could capture more energy from it. In the wave characteristic data, we choose 1.25m wave significant height to be constant for South coast of Tasmania in Australia. Again 1.25m constant wave height for Belgian coastal area of the North Sea in Belgium. For Adjacent seas which includes the Bohai Sea, Yellow Sea, East China Sea, as well as the Northern South China sea in China 3.25m wave significant height to be constant. 1.40m wave height to be constant for Shelf seas of India. And lastly, in the wave data of Pantelleria Island, Sicily, Italy 1.97m is considered as constant for the calculation purpose of incoming wave power effect on wave period.

4.2.2 Effect Of Incoming Wave Power On Wave Height

Table 4.3: Effect of incoming wave power on wave height while keeping the wave period constant.

Country	*h*(m)	*T*(s)	*H*(m)	Incoming Wave Power (Watt)
Australia *South coast of Tasmania (Oceania)*[38]	50	5.00	0.75 1.25 1.75 2.50 3.25 4.25 5.25 5.75 6.25	2754 7650 14995 30602 51717 88439 134953 161882 191260
Belgium *Belgian coastal area of the North Sea(Europe)*[39]	22	4.00	0.25 1.25 2.50 3.75	242 6054 24215 54483
China *Adjacent seas which includes the Bohai Sea, Yellow Sea, East China Sea, as well as the Northern South China sea (Asia)* [41][42]	50	7.60	3.10 3.25 2.65 2.60 2.45 2.90 3.40 3.35	69320 76191 50656 48762 43298 60664 83386 80952
India *Shelf seas of India(Asia)*[43][44]	71	7.46	1.30 1.40 1.13 1.50 0.90 0.80 1.00	12173 14118 9198 16207 5835 4610 7203
Italy *Pantelleria Island, Sicily* [45]	32	6.44	1.18 1.97 0.67 0.68 1.36 2.20 1.45 1.99 0.69	8487 23654 2736 2818 11273 29499 12814 24136 2902

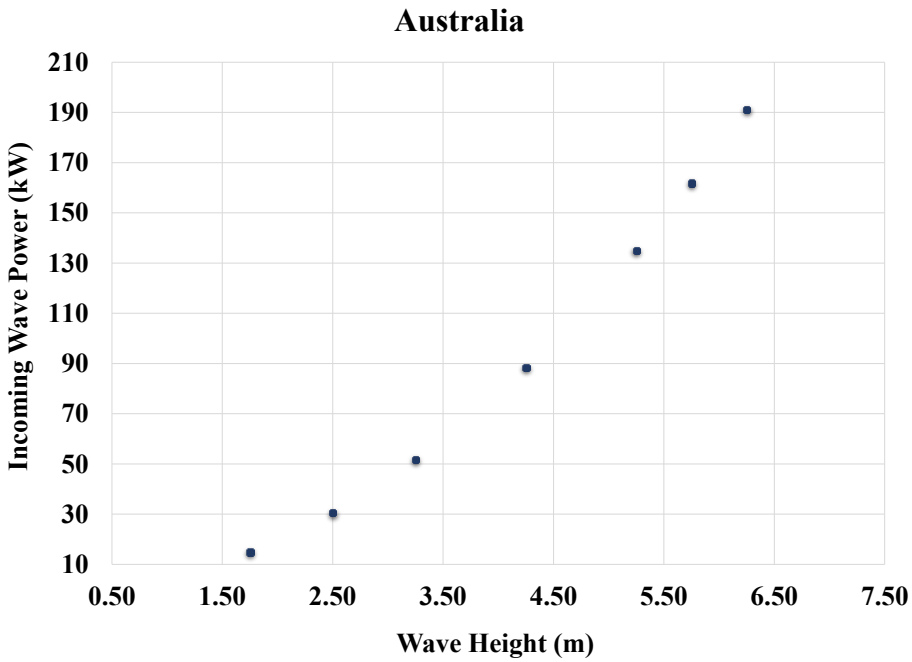

Figure 4.6: Effect of incoming wave power on wave height while keeping the wave period constant (**Australia** South coast of Tasmania).

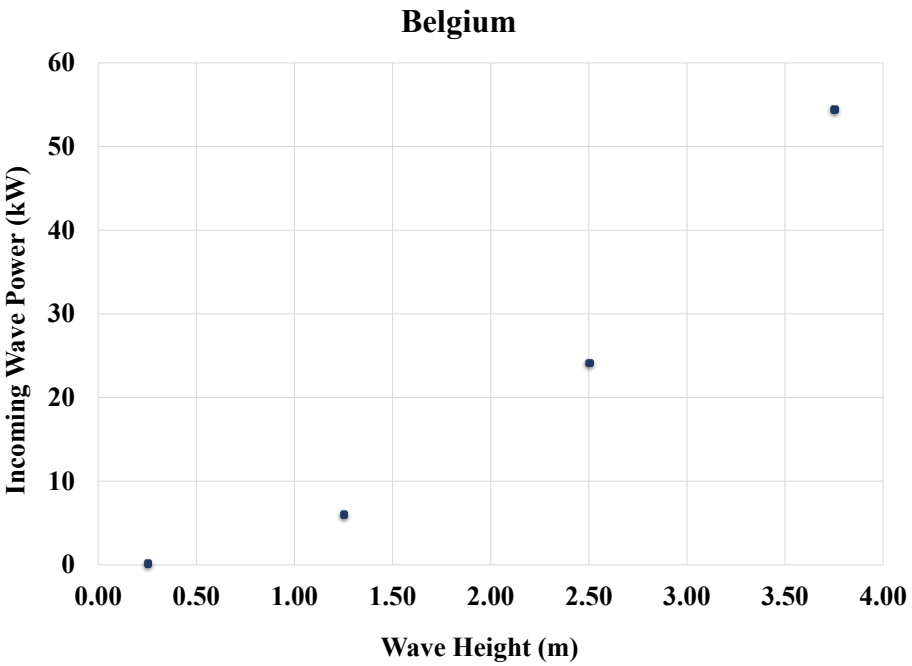

Figure 4.7: Effect of incoming wave power on wave height while keeping the wave period constant (**Belgium** Belgian coastal area of the North Sea).

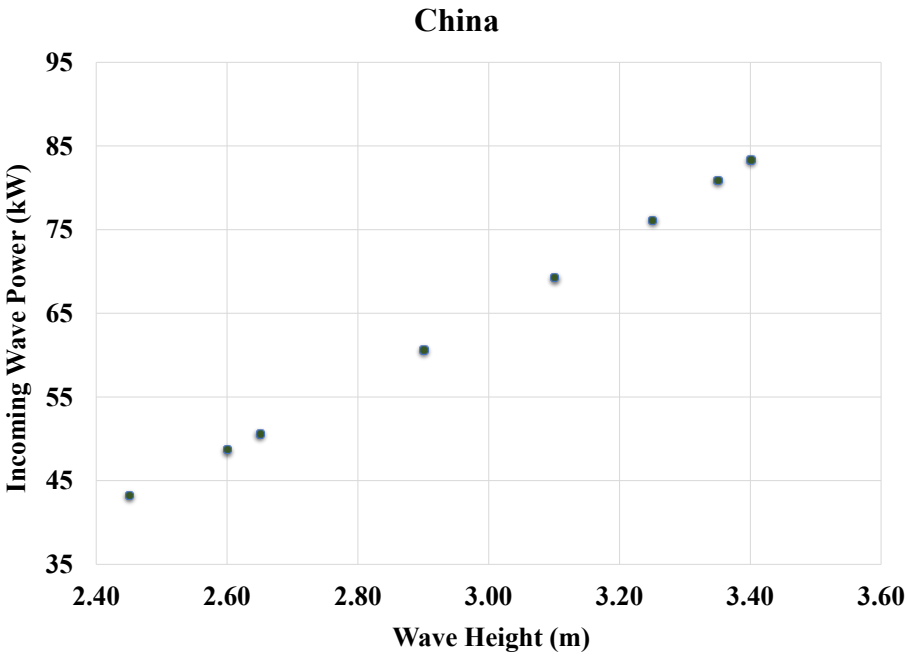

Figure 4.8: Effect of incoming wave power on wave height while keeping the wave period constant (**Italy** Pantelleria Island, Sicily).

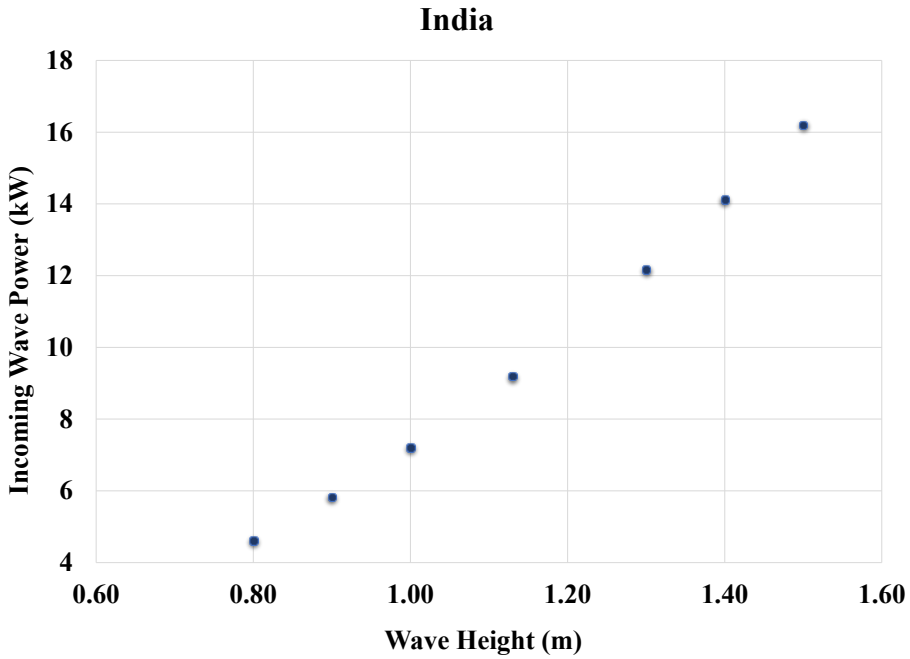

Figure 4.9: Effect of incoming wave power on wave height while keeping the wave period constant (**India** Shelf seas of India).

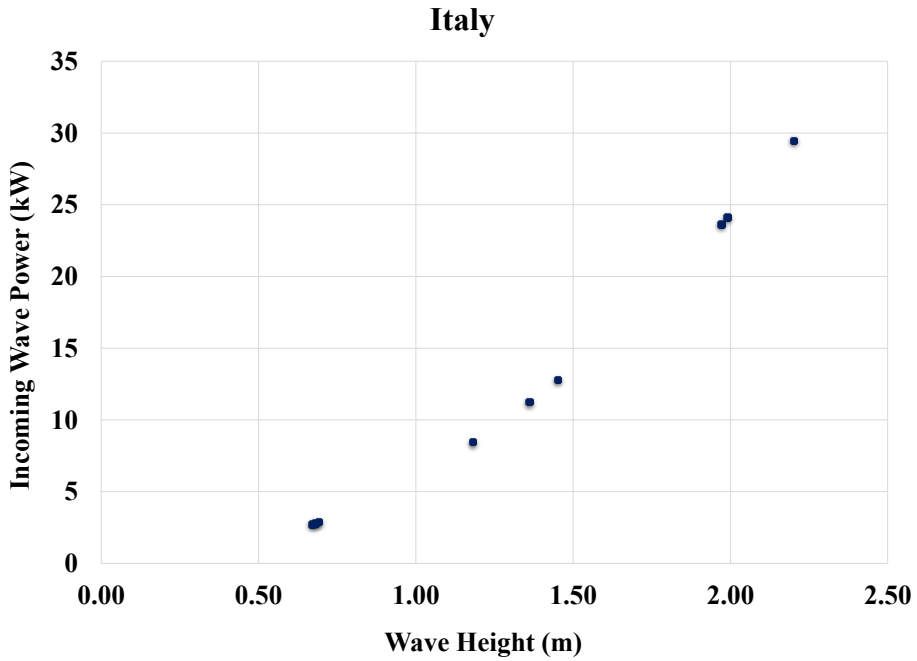

Figure 4.10: Effect of incoming wave power on wave height while keeping the wave period constant (**Italy** Pantelleria Island, Sicily).

In the above Figure 4.6- Figure 4.10, the graphs were plotted with the help of Equation 28 and 29 which also shows a linear relationship with the two parameters in each of them. The graphs were plotted by using data from Table 4.3. Increasing the wave height may increase the incoming wave power to the ***Wave Carpet***. In the wave characteristic data, we choose 5 sec wave period to be constant for South coast of Tasmania in Australia. Again 4 sec constant wave period for Belgian coastal area of the North Sea in Belgium. For Adjacent seas which includes the Bohai Sea, Yellow Sea, East China Sea, as well as the Northern South China sea in China 7.60 sec wave period to be constant. 7.46 sec wave period to be constant for Shelf seas of India. And lastly, in the wave data

of Pantelleria Island, Sicily, Italy 6.44 sec is considered as constant for the calculation purpose of incoming wave power effect on wave significant height.

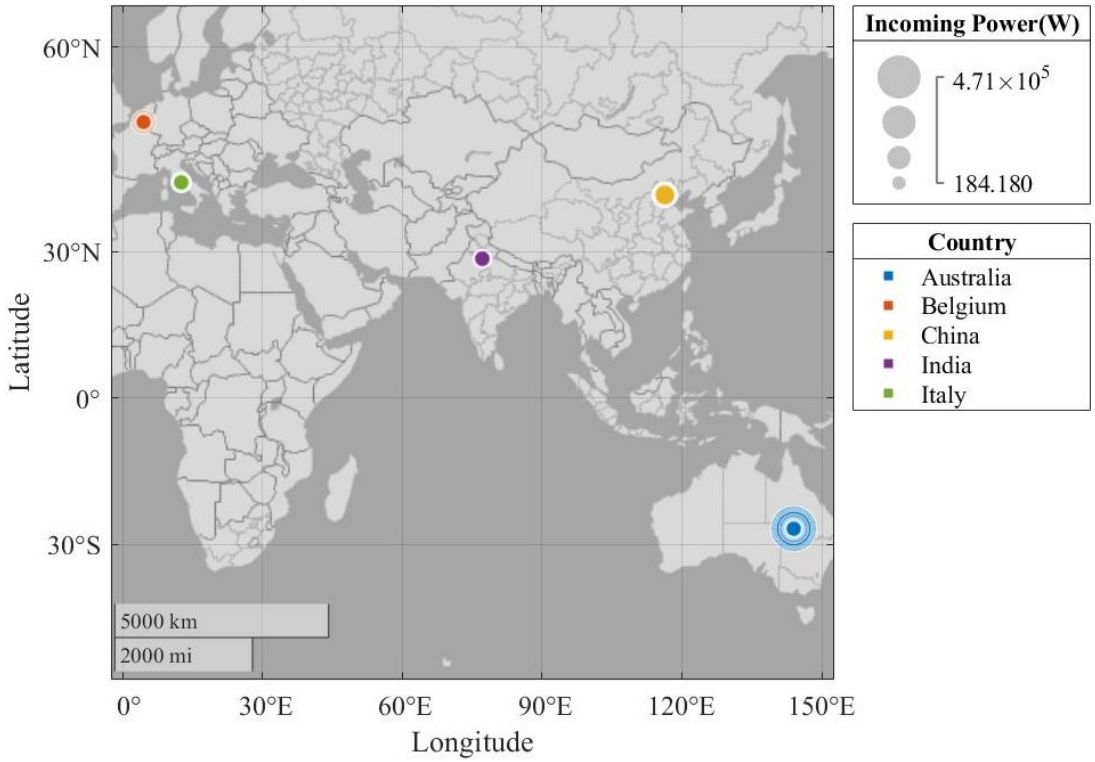

Figure 4.11: A geographical graph shows different range of Incoming Wave Power (Watt) to the ***Wave Carpet*** according to the coastal regions of some selected countries.

From Figure 4.11, it can be visualized that the incoming wave power to the ***Wave Carpet*** is higher in the coastal region of Australia which is approximately 471.261kW when the wave period is 12 sec, significant wave height is 6.25m, water dept is 50m, wave amplitude is 3.125m. The size of the circle represents the amount of incoming power to the Wave Carpe. The smaller size circle can be seen in India and the larger one can be seen in Australia. The smaller amount of incoming power in India is approximately 3.699 kW when the wave period is 5.90s, wave significant height is 0.80 m, water depth is 71m, wave amplitude is 0.4m.

Hence, using the Equation 28 and 29 along with Table 4.1, the graph plotted in Figure 4.11 can be achieved.

4.3 Energy Extraction by the *Wave carpet*

For one period of time the amount of energy, the carpet extracts in Equation 27 is shown where energy extraction from the ***Wave Carpet*** changes with different values[18] of ζ and γ. We can see the significant changes of energy extraction according to different geographical locations (where γ=0.9 and ζ=0.35) in following tables and figures.

4.3.1 Variation of dimensionless restoring force (γ=0.5 and 0.9) with dimensionless damping ratio (ζ =0.35-0.6) for Australia.

Table 4.4: Effect of energy extraction by ***Wave Carpet*** on dimensionless damping ratio while keeping the dimensionless restoring force γ=0.5 in case of Australia.

Coastal region of selected country	**Energy Extraction by *Wave Carpet* (Watt) when γ=0.5**							
	***T*(s)**	***H*(m)**	**ζ =0.35**	**ζ=0.40**	**ζ=0.45**	**ζ=0.50**	**ζ=0.55**	**ζ=0.60**
Australia *South coast of Tasmania (Oceania)* [38]	4.00	0.75	355.23	355.23	355.23	355.23	355.23	355.23
	5.00	1.25	986.73	986.734	986.74	986.74	986.74	986.73
	6.00	1.75	1930.36	1930.82	1931.19	1931.47	1931.71	1930.36
	7.00	2.5	3818.28	3834.59	3847.22	3857.31	3865.54	3818.28
	8.00	3.25	5388.52	5542.43	5663.16	5760.43	5840.51	5388.52
	9.00	4.25	5276.56	5896.33	6400.74	6819.73	7173.54	5276.56
	10.00	5.25	2.16	2979.37	3876.59	4682.09	5405.14	2.164
	11.00	5.75	53.38	10.959	1.46	0.19	0.025	53.39
	12.00	6.25	89.96	31.69	10.33	2.91	0.65	89.96
Average			1989.02	2396.46	2563.62	2710.67	2839.89	3198.09

Table 4.5: Effect of energy extraction by ***Wave Carpet*** on dimensionless damping ratio while keeping the dimensionless restoring force γ=0.9 in case of Australia.

Coastal region of selected country	**Energy Extraction by *Wave Carpet* (Watt) when γ=0.9**							
	***T*(s)**	***H*(m)**	**ζ =0.35**	**ζ=0.40**	**ζ=0.45**	**ζ=0.50**	**ζ=0.55**	**ζ=0.60**
Australia *South coast of Tasmania (Oceania)* [38]	4.00	0.75	362.75	361.48	360.48	359.68	359.04	358.52
	5.00	1.25	1014.07	1010.09	1006.78	1004.04	1001.77	999.88
	6.00	1.75	1996.50	1988.45	1981.49	1975.53	1970.45	1966.13
	7.00	2.5	4043.38	4026.45	4012.01	3999.82	3989.61	3981.06
	8.00	3.25	6477.57	6437.16	6406.92	6385.05	6369.92	6360.08
	9.00	4.25	9671.01	9537.22	9443.98	9383.78	9349.95	9336.69
	10.00	5.25	11664.67	11306.66	11053.48	10886.19	10788.10	10744.97
	11.00	5.75	9803.39	9207.00	8776.80	8480.73	8292.29	8189.79
	12.00	6.25	7465.75	6693.17	6133.45	5739.31	5474.68	5311.96
Average			5833.23	5618.63	1006.78	5357.13	5288.42	5249.90

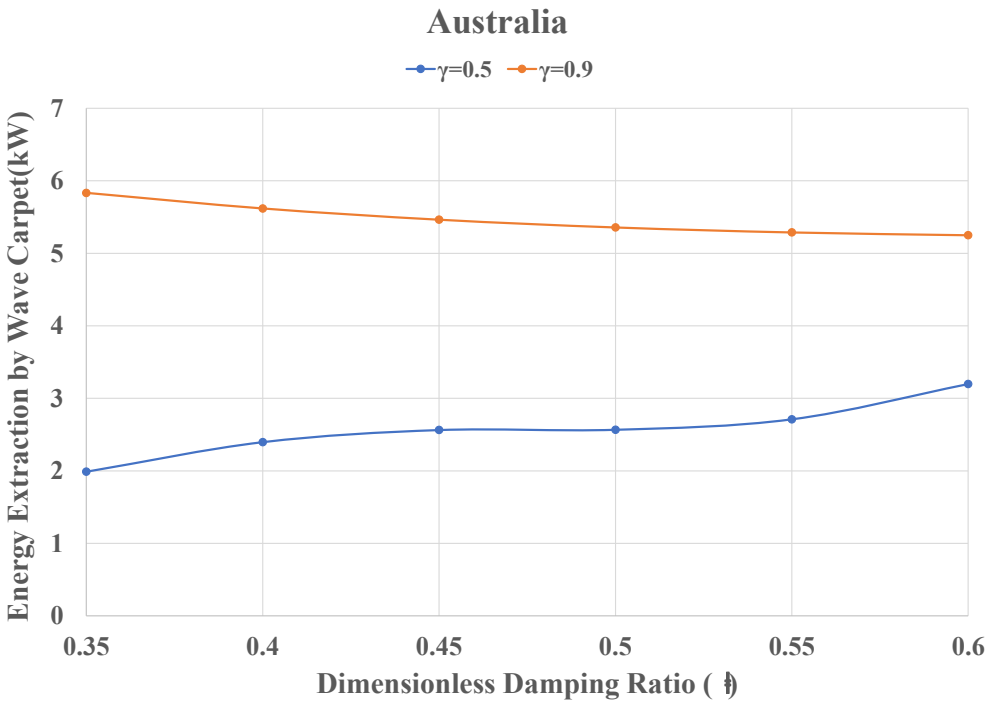

Figure 4.12: Effect of Energy (kW) Extracted by ***Wave Carpet*** (in coastal region of Australia) with γ =0.5,0.9 on dimensionless damping ratio (ζ =0.35-0.6).

The above Figure 4.12 can be achieved by using Table 4.4 – Table 4.5 which can be obtained from Equation 27. The average values of Table 4.4 and Table 4.5 are used to plot the graph in Figure 4.12. In case of Australia, when $\gamma = 0.9$, $\zeta = 0.35$ the energy extraction becomes higher. In another word, when $\gamma=0.5$, $\zeta=0.6$ the outcomings are higher. The dimensionless damping ratio (ζ) is a vital property of double acting damper of the ***Wave Carpet***. Hence, exploratory the variation of ζ might give a perspective of implanting ***Wave Carpet*** to the selective coastal areas.

4.3.2 Variation of dimensionless restoring force (γ=0.5 and 0.9) with dimensionless damping ratio (ζ =0.35-0.6) for Belgium.

Table 4.6: Effect of energy extraction by ***Wave Carpet*** on dimensionless damping ratio while keeping the dimensionless restoring force γ=0.5 in case of Belgium.

Coastal region of selected country	**Energy Extraction by *Wave Carpet* (Watt) when γ=0.5**							
	***T*(s)**	***H*(m)**	**ζ =0.35**	**ζ=0.40**	**ζ=0.45**	**ζ=0.50**	**ζ=0.55**	**ζ=0.60**
Belgium *Belgian coastal area of the North Sea (Europe)* [39]	3.00 4.00 5.00 6.00	0.25 1.25 2.50 3.75	39.47 985.09 3674.63 4933.23	39.47 985.30 3709.29 5380.69	39.47 985.47 3736.11 5734.19	39.47 985.59 3757.48 6021.34	39.47 985.70 3774.92 6259.60	39.46 985.79 3789.40 6460.68
Average			2408.10	2528.68	2623.81	2700.97	2764.92	2818.84

Table 4.7: Effect of energy extraction by ***Wave Carpet*** on dimensionless damping ratio while keeping the dimensionless restoring force γ=0.9 in case of Belgium.

Coastal region of selected country	**Energy Extraction by *Wave Carpet* (Watt) when γ=0.9**							
	***T*(s)**	***H*(m)**	**ζ =0.35**	**ζ=0.40**	**ζ=0.45**	**ζ=0.50**	**ζ=0.55**	**ζ=0.60**
Belgium *Belgian coastal area of the North Sea (Europe)* [39]	3.00 4.00 5.00 6.00	0.25 1.25 2.50 3.75	40.44 1018.88 4002.23 7947.14	40.29 1014.77 3983.96 7857.16	40.16 1011.21 3968.83 7792.31	39.47 985.59 3757.48 6021.34	39.98 1005.56 3946.39 7720.94	39.92 1003.34 3938.29 7706.93
Average			3252.17	3224.05	3203.13	3188.22	3178.22	3172.12

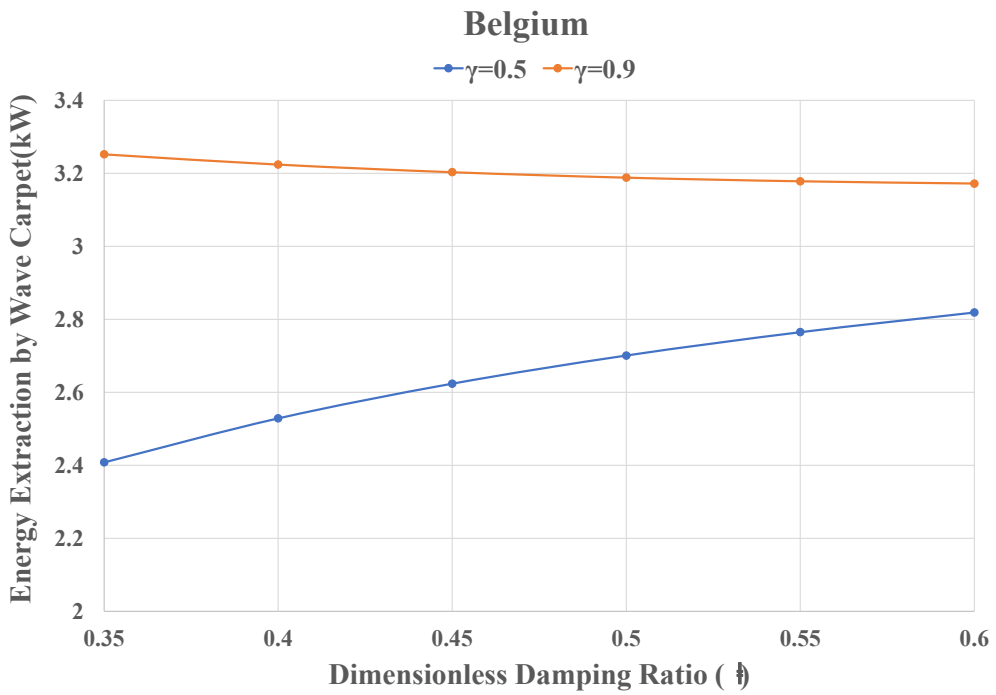

Figure 4.13: Effect of Energy (kW) Extracted by ***Wave Carpet*** (in coastal region of Belgium) with γ =0.5,0.9 on dimensionless damping ratio (ζ =0.35-0.6).

The above Figure 4.13 can be achieved by using Table 4.6 – Table 4.7 which can be obtained from Equation 27. The average values of Table 4.6 and Table 4.7 are used to plot the graph in Figure 4.13. In case of Belgium, when γ = 0.9, ζ =0.35 the energy extraction becomes higher. In another word, when γ=0.5, ζ=0.6 the outcomings are higher where the increment of values is faster. They follow the same graph trend as Australia does. The dimensionless damping ratio (ζ) is a vital property of double acting damper of the ***Wave Carpet***. Hence, exploratory the variation of ζ might give a perspective of implanting ***Wave Carpet*** to the selective coastal areas.

4.3.3 Variation of dimensionless restoring force (γ=0.5 and 0.9) with dimensionless damping ratio (ζ =0.35-0.6) for China.

Table 4.8: Effect of energy extraction by ***Wave Carpet*** on dimensionless damping ratio while keeping the dimensionless restoring force γ=0.5 in case of China.

Coastal region of selected country	**Energy Extraction by *Wave Carpet* (Watt) when γ=0.5**							
	***T*(s)**	***H*(m)**	**ζ =0.35**	**ζ=0.40**	**ζ=0.45**	**ζ=0.50**	**ζ=0.55**	**ζ=0.60**
China *Adjacent seas (Asia)* [41][42]	7.70	3.10	5330.11	5421.17	5492.19	5549.13	5595.81	5634.79
	7.60	3.25	6003.62	6086.55	6151.09	6202.75	6245.04	6280.31
	6.90	2.65	4324.47	4338.50	4349.36	4358.03	4365.09	4370.97
	7.05	2.60	4115.45	4134.91	4149.98	4162.01	4171.84	4180.01
	7.55	2.45	3396.84	3445.48	3483.40	3513.80	3538.71	3559.51
	7.93	2.90	4352.75	4468.01	4558.39	4631.20	4691.13	4741.33
	8.35	3.40	5096.06	5348.55	5548.67	5711.3	5846.16	5959.82
	8.40	3.35	4801.67	5060.70	5266.50	5434.07	5573.24	5690.70
Average			4677.62	4787.98	4874.95	4945.29	5003.38	5052.18

Table 4.9: Effect of energy extraction by ***Wave Carpet*** on dimensionless damping ratio while keeping the dimensionless restoring force γ=0.9 in case of China.

Coastal region of selected country	**Energy Extraction by *Wave Carpet* (Watt) when γ=0.9**							
	***T*(s)**	***H*(m)**	**ζ =0.35**	**ζ=0.40**	**ζ=0.45**	**ζ=0.50**	**ζ=0.55**	**ζ=0.60**
China *Adjacent seas (Asia)* [41][42]	7.70	3.10	6037.44	6006.04	5981.43	5962.52	5948.27	5937.78
	7.60	3.25	6685.85	6652.97	6626.69	6606.02	6590.01	6577.77
	6.90	2.65	4554.68	4535.87	4519.70	4505.94	4494.29	4484.48
	7.05	2.60	4368.78	4350.36	4334.70	4321.54	4310.53	4301.36
	7.55	2.45	3791.22	3772.44	3757.56	3745.96	3737.06	3730.35
	7.93	2.90	5175.79	5144.51	5121.01	5103.91	5091.97	5084.09
	8.35	3.40	6813.52	6757.84	6717.95	6690.94	6674.18	6665.40
	8.40	3.35	6561.87	6505.59	6465.54	6438.69	6422.33	6414.13
Average			5498.64	5465.70	5440.57	5421.94	5408.58	5399.42

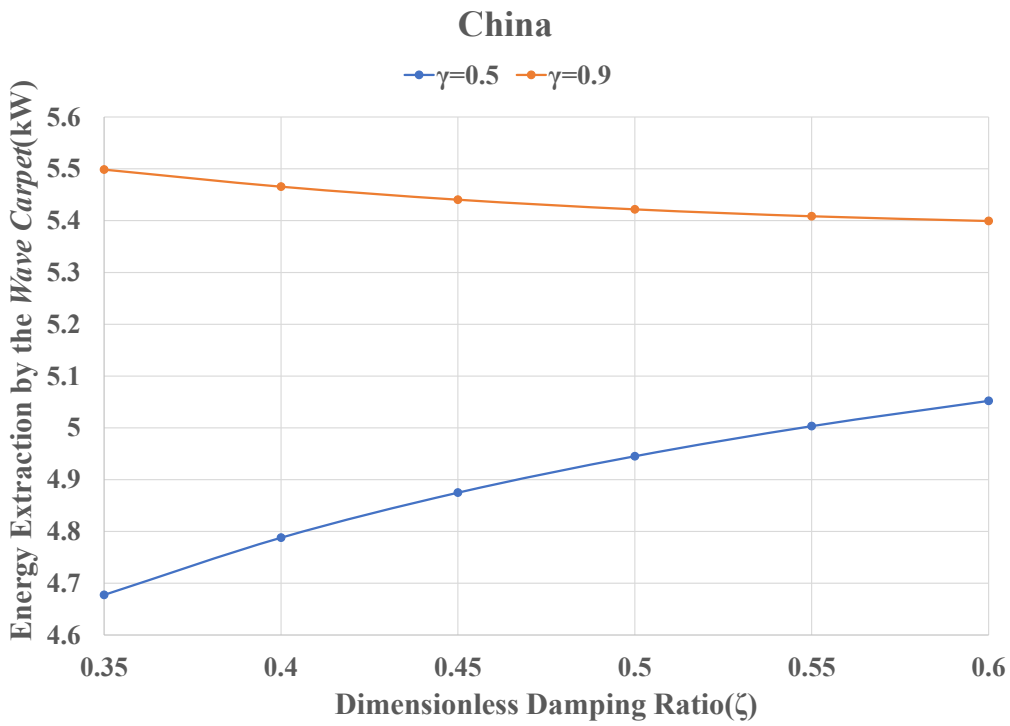

Figure 4.14: Effect of Energy (kW) Extracted by ***Wave Carpet*** (in coastal region of China) with γ =0.5,0.9 on dimensionless damping ratio (ζ =0.35-0.6).

The above Figure 4.14 can be achieved by using Table 4.8 – Table 4.9 which can be obtained from Equation 27. The average values of Table 4.8 and Table 4.9 are used to plot the graph in Figure 4.14. In case of China, when γ = 0.9, ζ =0.35 the energy extraction becomes higher. In another word, when γ=0.5, ζ=0.6 the outcomings are higher which is similar to Australia and Belgium cases. They follow the same graph trend as Australia and Belgium do. The dimensionless damping ratio (ζ) is a vital property of double acting damper of the ***Wave Carpet***. Hence, exploratory the variation of ζ might give a perspective of implanting ***Wave Carpet*** to the selective coastal areas.

4.3.4 Variation of dimensionless restoring force (γ=0.5 and 0.9) with dimensionless damping ratio (ζ =0.35-0.6) for India.

Table 4.10: Effect of energy extraction by ***Wave Carpet*** on dimensionless damping ratio while keeping the dimensionless restoring force γ=0.5 in case of India

Coastal region of selected country	**Energy Extraction by *Wave Carpet* (Watt) when γ=0.5**							
	***T*(s)**	***H*(m)**	**ζ =0.35**	**ζ=0.40**	**ζ=0.45**	**ζ=0.50**	**ζ=0.55**	**ζ=0.60**
India *Shelf seas of India (Asia)* [43][44]	7.63	1.30	1099.75	1095.30	1091.45	1088.15	1085.35	1082.97
	7.46	1.40	1276.83	1271.67	1267.21	1263.38	1260.11	1257.33
	7.90	1.13	827.877	824.48	821.57	819.12	817.049	815.31
	7.80	1.50	1462.41	1456.46	1451.33	1446.95	1443.23	1440.08
	5.60	0.90	524.744	522.73	521.08	519.73	518.62	517.71
	5.90	0.80	415.243	413.618	412.27	411.15	410.23	409.47
	6.80	1.00	651.25	648.64	646.39	644.48	642.87	641.51
Average			860.16	861.21	862.03	862.68	863.21	863.66

Table 4.11: Effect of energy extraction by ***Wave Carpet*** on dimensionless damping ratio while keeping the dimensionless restoring force γ=0.9 in case of India.

Coastal region of selected country	**Energy Extraction by *Wave Carpet* (Watt) when γ=0.9**							
	***T*(s)**	***H*(m)**	**ζ =0.35**	**ζ=0.40**	**ζ=0.45**	**ζ=0.50**	**ζ=0.55**	**ζ=0.60**
India *Shelf seas of India (Asia)* [43][44]	7.63	1.30	1099.75	1095.30	1091.45	1088.15	1085.35	1082.97
	7.46	1.40	1276.83	1271.67	1267.21	1263.38	1260.11	1257.33
	7.90	1.13	827.87	824.48	821.57	819.12	817.04	815.31
	7.80	1.50	1462.41	1456.46	1451.33	1446.95	1443.23	1440.08
	5.60	0.90	524.74	522.73	521.08	519.73	518.62	517.71
	5.90	0.80	415.24	413.62	412.27	411.15	410.23	409.47
	6.80	1.00	651.25	648.63	646.39	644.48	642.87	641.51
Average			894.01	890.42	887.33	884.71	882.49	880.63

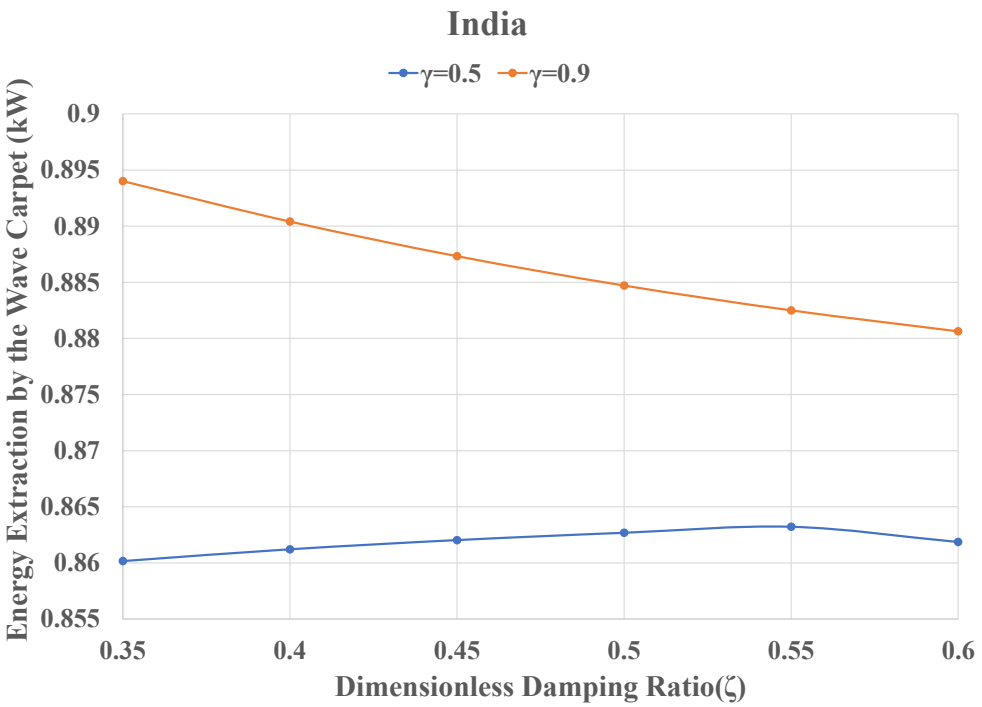

Figure 4.15: Effect of Energy (kW) Extracted by ***Wave Carpet*** (in coastal region of India) with γ =0.5,0.9 on dimensionless damping ratio (ζ =0.35-0.6).

The above Figure 4.15 can be achieved by using Table 4.10 – Table 4.11 which can be obtained from Equation 27. The average values of Table 4.10 and Table 4.11 are used to plot the graph in Figure 4.15. In case of India, when γ = 0.9, ζ =0.35 the energy extraction becomes higher. In another word, when γ=0.5, ζ=0.6 the outcomings are trend to decrease which is not similar to Australia and Belgium cases. They are not following the same graph trend as Australia and Belgium do. But when γ=0.5 and ζ=0.55, the outcomings become higher. The dimensionless damping ratio (ζ) is a vital property of double acting damper of the ***Wave Carpet***. Hence, exploratory the variation of ζ might give a perspective of implanting ***Wave Carpet*** to the selective coastal areas.

4.3.5 Variation of dimensionless restoring force (γ=0.5 and 0.9) with dimensionless damping ratio (ζ =0.35-0.6) for Italy

Table 4.12: Effect of energy extraction by ***Wave Carpet*** on dimensionless damping ratio while keeping the dimensionless restoring force γ=0.5 in case of Italy.

Coastal region of selected country	**Energy Extraction by *Wave Carpet* (Watt) when γ=0.5**							
	***T*(s)**	***H*(m)**	**ζ =0.35**	**ζ=0.40**	**ζ=0.45**	**ζ=0.50**	**ζ=0.55**	**ζ=0.60**
Italy *Pantelleria Island, Sicily(Europe)*[45]	5.31	1.18	866.27	867.93	869.22	870.24	870.24	871.76
	6.44	1.97	1932.43	1994.08	2042.55	2081.67	2081.67	2140.97
	7.38	0.67	39.21	52.29	64.59	75.99	75.99	96.12
	6.54	0.68	179.74	191.56	201.13	209.03	209.03	221.33
	6.83	1.36	648.34	702.12	745.79	781.95	781.95	838.40
	8.09	2.20	0.07	0.0047	396.68	514.35	514.35	731.02
	7.77	1.45	126.21	185.85	243.07	296.80	296.80	392.86
	7.27	1.99	924.74	1068.17	1187.87	1289.23	1289.23	1451.46
	5.36	0.69	293.79	294.66	295.33	295.87	295.87	296.67
Average			556.76	595.18	671.80	712.79	749.42	782.29

Table 4.13: Effect of energy extraction by ***Wave Carpet*** on dimensionless damping ratio while keeping the dimensionless restoring force γ=0.9 in case of Italy

Coastal region of selected country	**Energy Extraction by *Wave Carpet* (Watt) when γ=0.9**							
	***T*(s)**	***H*(m)**	**ζ =0.35**	**ζ=0.40**	**ζ=0.45**	**ζ=0.50**	**ζ=0.55**	**ζ=0.60**
Italy *Pantelleria Island, Sicily(Europe)*[45]	5.31	1.18	905.51	910.83	898.65	895.91	893.59	891.61
	6.44	1.97	2362.98	2347.52	2336.08	2327.94	2322.44	2319.02
	7.38	0.67	175.80	170.48	166.97	164.90	163.95	163.86
	6.54	0.68	260.25	257.74	256.07	255.04	254.52	254.39
	6.83	1.36	1021.35	1009.87	1002.04	997.13	994.52	993.67
	8.09	2.20	1761.62	1690.44	1640.64	1608.08	1589.28	1581.3
	7.77	1.45	806.92	779.02	759.93	747.88	741.42	739.32
	7.27	1.99	2002.63	1968.81	1945.60	1930.99	1923.22	1920.76
	5.36	0.69	308.67	307.41	306.32	305.39	304.62	303.97
Average			1067.30	1049.12	1034.70	1025.92	1020.84	1018.66

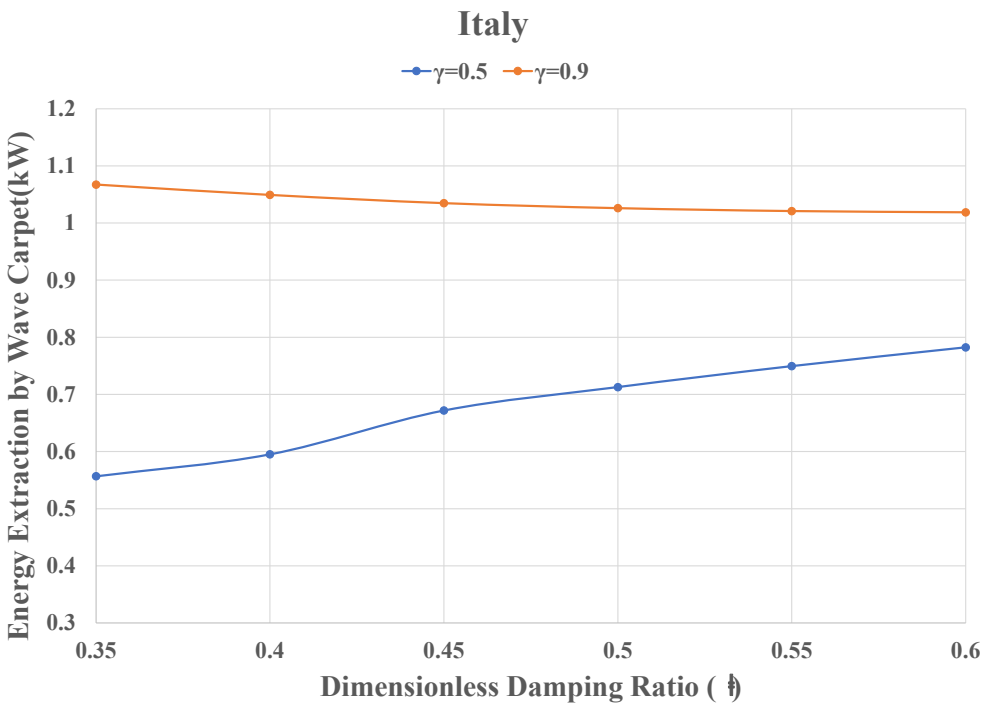

Figure 4.16: Effect of Energy (kW) Extracted by ***Wave Carpet*** (in coastal region of Italy) with γ =0.5,0.9 on dimensionless damping ratio (ζ =0.35-0.6).

The above Figure 4.16 can be achieved by using Table 4.12 – Table 4.13 which can be obtained from Equation 27. The average values of Table 4.12 and Table 4.13 are used to plot the graph in Figure 4.16. In case of Italy, when $\gamma = 0.9$, $\zeta = 0.35$ the energy extraction becomes higher. In another word, when $\gamma=0.5$, $\zeta=0.6$ the outcomings are higher which is similar to Australia and Belgium cases. They follow the same graph trend as Australia and Belgium do. The dimensionless damping ratio (ζ) is a vital property of double acting damper of the ***Wave Carpet***. Hence, exploratory the variation of ζ might give a perspective of implanting ***Wave Carpet*** to the selective coastal areas.

4.3.6 Overall View of Energy Extraction by *Wave Carpet*

Table 4.14: Average vale of energy extraction by the ***Wave Carpet*** when $\gamma=0.9$, $\zeta=0.35$

Coastal regions of selected countries	**Country Latitude**	**Country Longitude**	**Average value of Energy (Watt)Extraction by *Wave Carpet* when ($\gamma=0.9$, $\zeta=0.35$)**
Australia [38]	-27	144	5833.23
Belgium [39]	50.85	4.35	3252.17
China [41][42]	39.91667	116.3833	5498.64
India [43][44]	28.61389	77.20833	894.01
Italy [45]	41.9	12.48333	1067.31

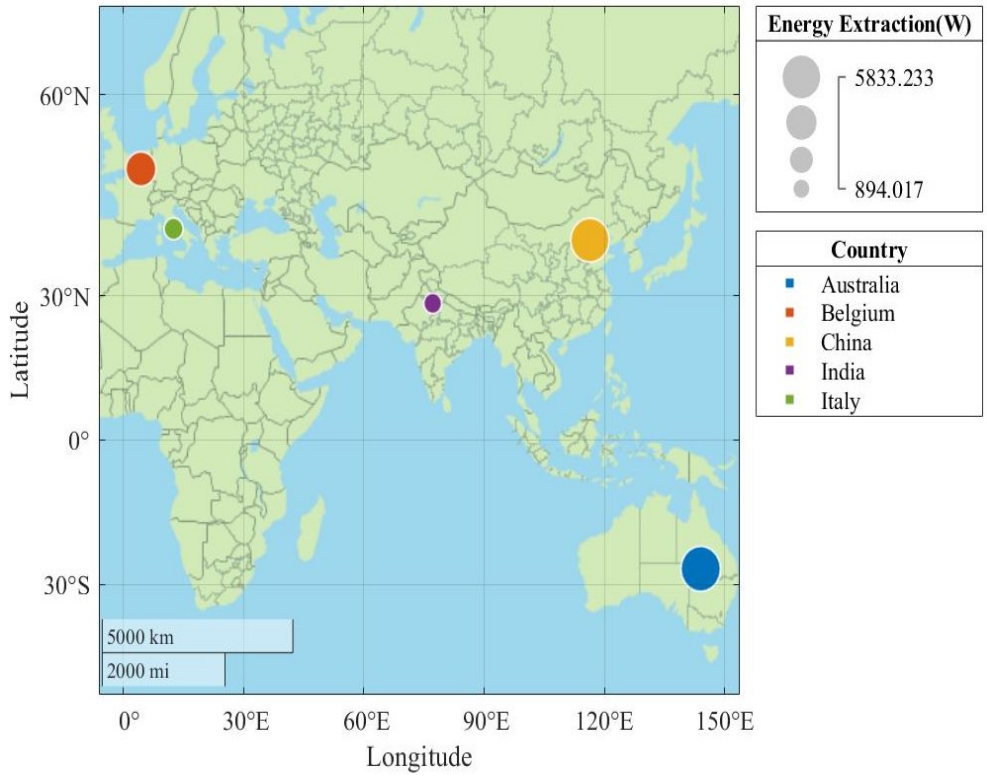

Figure 4.17: A geographical graph shows wave energy extraction by the ***Wave Carpet*** according to some coastal areas of countries of selected countries when γ=0.9, ζ=0.35.

With the help of Table 4.14, Figure 4.17 can be plot by using Equation 27. Overall, of the variation we get the higher value of energy extraction at γ=0.9, ζ=0.35. from this perspective the Figure 4.17 is plotted to visualize the energy extraction to the selected coastal regions of the countries. It can also be visualized that the energy extraction by the ***Wave Carpet*** is higher in the coastal region of Australia which is approximately 5833.233W when the wave properties are taken as an average. The size of the circle represents the amount of the energy extraction by the ***Wave Carpet*** Wave Carpe. The smaller size circle can be seen in India and the larger one can be seen in Australia. The smaller amount of energy extraction in India which is approximately 894.0167W when the wave properties are taken as an average. Hence, using the Equation 27 along with Table 14, the graph plotted in Figure 4.20 can be achieved where γ=0.9, ζ=0.35.

Chapter 5 Conclusion and Future plan

5.1 Conclusion

Wave energy is a green energy medium which has a lot of potential. As a result, this green energy could solve a huge energy crisis which is a crying issue nowadays. Utilizing wave energy in field wherever possible many author gave positive opinion on wave potential. Among them Prof. Reza Alam gave instructions on extracting wave energy by using a ***Wave Carpet*** and also provided an empirical solution for a synthetic seafloor carpet's motion supported by multiple springs and generators. In this study, the authors have shown the ability of extracting wave energy by the ***Wave Carpet*** and incoming power to the ***Wave Carpet*** in selective coastal regions of Australia, Belgium, China, India, Italy. This paper includes a detailed analysis of wave energy extraction by the ***Wave Carpet*** in order to satisfy energy demand on reliability on renewable energy sources. We have some key findings of this entire project, they are:

- Dimensionless damping ratio (ζ) and dimensionless restoring force (γ) are considered as 0.35, 0.6 and 0.1, 0.5, 0.9 [18]. It is noted that, the higher value of dimensionless restoring force and lower value of dimensionless damping ratio will give the higher rate of energy extraction. Although in this study dimensionless restoring force as 0.1 won't be counted as the results were not relevant according to the collected data.
- Calculated Wave energy extraction by the Wave Carpet is also higher in the selective coastal region of Australia which is approximately **11.664 kW** when $\gamma = 0.9$ and $\zeta = 0.35$.

- Another finding of our study was the energy extraction by the Wave Carpet is lower in the coastal region of India which is approximately **404.1656 W** when $\gamma = 0.5$ and $\zeta = 0.35$.

There may have some limitation with this project, that is the power and energy extraction calculation associated with ***Wave Carpet*** solely derived from available wave data of the few selective countries rather than the actual field measurements. The compilation of real wave data, as well as the validation of the Wave Carpet model, is a major analysis in and of itself, and it is beyond the reach of this review. For this reason, the authors were unable to perform a detailed analysis into the validity of the available wave data by comparing it to the field or laboratory measurements. Moreover, an introductory idea could be obtained from the result produced in this study in case of planning and installation of actual ***Wave Carpet***. The ***Wave Carpet*** efficiency is not satisfactory in the selected places as well as the incoming power and energy extraction are also less than the required demand for energy in this study.

5.2 Future Plan

The next phase of our work will be improving the ***Wave Carpet*** efficiency. The ***Wave Carpet*** could be more satisfactory in the selected places if the Break- water might be incorporated with the ***Wave Carpet***, so that it could provide shore- protection as well.

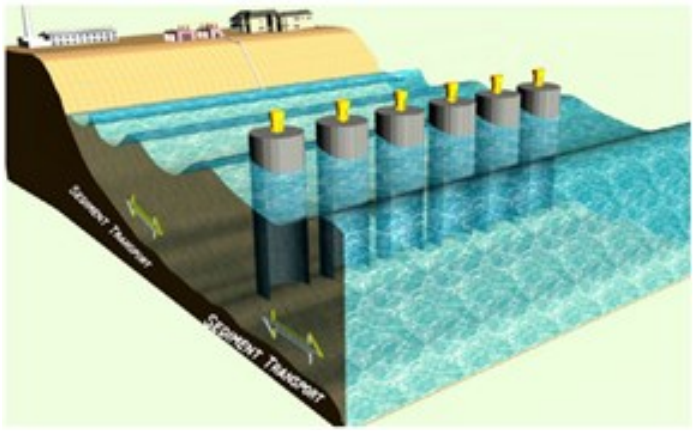

Figure 5.1: Oscillating Water Column (OWC) is a type of pile breakwater[46]

The findings of our work could be promoting close collaboration between wave energy utilization community by using ***Wave Carpet*** and the shore protection community by using OWC for profitable-scale settlement of wave energy converters and contribute to making wave potential enormously competitive.

Chapter 6 Bibliography

[1] T. Shahriar, M. Shahrear, and A. Hossain, "ISLAMIC UNIVERSITY OF TECHNOLOGY (IUT) Department of Mechanical and Chemical Engineering Islamic University of Technology (IUT) NOVEMBER 2018," no. November, 2018.

[2] M. Fadaeenejad, R. Shamsipour, S. D. Rokni, and C. Gomes, "New approaches in harnessing wave energy : With special attention to small islands," *Renew. Sustain. Energy Rev.*, vol. 29, pp. 345–354, 2014, doi: 10.1016/j.rser.2013.08.077.

[3] R. H. Leeney, D. Greaves, D. Conley, A. Marie, and O. Hagan, "Ocean & Coastal Management Environmental Impact Assessments for wave energy developments e Learning from existing activities and informing future research priorities," *Ocean Coast. Manag.*, vol. 99, pp. 14–22, 2014, doi: 10.1016/j.ocecoaman.2014.05.025.

[4] P. Mccullen *et al.*, "Wave energy in Europe : current status and perspectives," vol. 6, pp. 405–431, 2002.

[5] C. Frid *et al.*, "The environmental interactions of tidal and wave energy generation devices," *Environ. Impact Assess. Rev.*, vol. 32, no. 1, pp. 133–139, 2012, doi: 10.1016/j.eiar.2011.06.002.

[6] T. Shahriar, M. A. Habib, M. Hasanuzzaman, and M. Shahrear-bin-zaman, "Modelling and optimization of Searaser wave energy converter based hydroelectric power generation for Saint Martin ' s Island in Bangladesh," *Ocean Eng.*, vol. 192, no. July, p. 106289, 2019, doi: 10.1016/j.oceaneng.2019.106289.

[7] H. Titah-benbouzid and M. Benbouzid, “Ocean Wave Energy Extraction : Up-to-Date Technologies Review and Evaluation,” 2014.

[8] L. (Uppsala U. Simon, “Buoy and Generator Interacation with Ocean Waves,” *2011*, no. 1, pp. 30–40, 2011.

[9] J. Hayward and P. Osman, “The potential of wave energy,” no. March, 2011.

[10] “chaine-flottante-articulee.” [Online]. Available: http://energies-marines-tpe-2016.e-monsite.com/album-photos/chaine-flottante-articulee.html. [Accessed: 11-Mar-2021].

[11] EMEC, “Wave devices : EMEC: European Marine Energy Centre.” 2014.

[12] “Wave Energy Converter Technologies #1 – Blackfish Engineering.” [Online]. Available: https://blackfishengineering.com/2018/02/26/wave-energy-converter-technologies-1/. [Accessed: 12-Mar-2021].

[13] Bureau of Ocean Energy Management, “Types of WEC - Water Science,” 2015. [Online]. Available: https://wave-energies.weebly.com/types-of-wec.html. [Accessed: 13-Mar-2021].

[14] C. Retzler, “Measurements of the slow drift dynamics of a model Pelamis wave energy converter,” in *Renewable Energy*, 2006, vol. 31, no. 2, pp. 257–269, doi: 10.1016/j.renene.2005.08.025.

[15] L. Volsun, “Searaser converts ocean wave power into clean renewable energy |

Energy | The Earth Times." [Online]. Available: http://www.earthtimes.org/energy/searaser-converts-ocean-wave-power-clean-renewable-energy/1776/. [Accessed: 13-Mar-2021].

[16] A. P. Stevens, "Ocean energy could be the wave of the future Science News for Students." [Online]. Available: https://www.sciencenewsforstudents.org/article/ocean-energy-could-be-wave-future. [Accessed: 13-Mar-2021].

[17] M. Lehmann, R. Elandt, H. Pham, R. Ghorbani, M. Shakeri, and M. Alam, "An artificial seabed carpet for multidirectional and broadband wave energy extraction : Theory and Experiment," *Proc. 10th Eur. Wave Tidal Energy Conf. EWTEC2013, 2-5 Sept. 2013, Aalborg, Denmark.*, 2013.

[18] M. Engineering, "Nonlinear analysis of an actuated seafloor-mounted carpet for a high-performance," no. March, pp. 3153–3171, 2012, doi: 10.1098/rspa.2012.0193.

[19] Rinkesh, "Various Advantages and Disadvantages of Wave Energy - Conserve Energy Future," *Conserve Energy Future*. [Online]. Available: https://www.conserve-energy-future.com/advantages_disadvantages_waveenergy.php. [Accessed: 13-Mar-2021].

[20] R. Pelc and R. M. Fujita, "Renewable energy from the ocean," vol. 26, no. June, pp. 471–479, 2002.

[21] M. N. Ayob, *Adaptation of wave power plants to regions with high tides*. 2019.

[22] T. Staedter, “Organovo - MIT Technology Review.” [Online]. Available: http://www2.technologyreview.com/tr50/organovo/. [Accessed: 13-Mar-2021].

[23] Blackfish Engineering, “Wave Energy Converter Technologies #5 – Blackfish Engineering.” [Online]. Available: https://blackfishengineering.com/2018/03/26/wave-energy-converter-technologies-5/. [Accessed: 13-Mar-2021].

[24] D. Mcginn *et al.*, *RenewableS 2013 GLOBAL STATUS REPORT 2013*. 2013.

[25] M. N. Uddin, M. A. Rahman, M. Mofijur, J. Taweekun, K. Techato, and M. G. Rasul, “ScienceDirect ScienceDirect Renewable energy in Symposium Bangladesh : Status and prospects Renewable energy in Bangladesh : Status and prospects function district,” *Energy Procedia*, vol. 160, pp. 655–661, 2019, doi: 10.1016/j.egypro.2019.02.218.

[26] S. Jacobsson and A. Johnson, “The di ! usion of renewable energy technology : an analytical framework and key issues for research,” vol. 28, 2000.

[27] P. S. Liss and P. G. Slater, “© 1974 Nature Publishing Group,” 1974.

[28] T. W. Thorpe, *A Brief Review of Wave Energy*. UK: Harwell Laboratory, Energy Technology Support Unit, 1999.

[29] B. Drew, A. R. Plummer, and M. N. Sahinkaya, “A review of wave energy converter technology,” vol. 223, pp. 887–902, 2009, doi: 10.1243/09576509JPE782.

[30] A. F. Seafloor, C. For, and W. E. Extraction, "Omae2012-84034," *ASME 2012 31st Int. ...*, 2012.

[31] "Wave power - Wikipedia." [Online]. Available: https://en.wikipedia.org/wiki/Wave_power. [Accessed: 13-Mar-2021].

[32] H. X. Li, D. J. Edwards, M. R. Hosseini, and G. P. Costin, "A review on renewable energy transition in Australia: An updated depiction," *J. Clean. Prod.*, vol. 242, p. 118475, 2020, doi: 10.1016/j.jclepro.2019.118475.

[33] A. Clément *et al.*, "Wave energy in Europe: Current status and perspectives," *Renew. Sustain. Energy Rev.*, vol. 6, no. 5, pp. 405–431, 2002, doi: 10.1016/S1364-0321(02)00009-6.

[34] D. Zhang, W. Li, Y. Lin, and J. Bao, "An overview of hydraulic systems in wave energy application in China," *Renew. Sustain. Energy Rev.*, vol. 16, no. 7, pp. 4522–4526, 2012, doi: 10.1016/j.rser.2012.04.005.

[35] R. P. Patel, G. Nagababu, S. V. V. Arun Kumar, M. Seemanth, and S. S. Kachhwaha, "Wave resource assessment and wave energy exploitation along the Indian coast," *Ocean Eng.*, vol. 217, no. July, p. 107834, 2020, doi: 10.1016/j.oceaneng.2020.107834.

[36] V. Sundar, *Ocean Wave Mechanics Applications in Marine Structures*, First. Chichester, West Sussex PO19 8SQ United Kingdom: John Wiley & Sons Ltd, 2016.

[37] C. Engineering, "SHORE PROTECTION MANUAL US Army Corps of Engineers,"

Coast. Eng., vol. I, 1984, doi: 10.5962/bhl.title.47830.

[38] E. Arzaghi, M. M. Abaei, R. Abbassi, M. O'Reilly, V. Garaniya, and I. Penesis, "A Markovian approach to power generation capacity assessment of floating wave energy converters," *Renew. Energy*, vol. 146, pp. 2736–2743, 2020, doi: 10.1016/j.renene.2019.08.099.

[39] M. Vantorre, R. Banasiak, and R. Verhoeven, "Modelling of hydraulic performance and wave energy extraction by a point absorber in heave," vol. 26, pp. 61–72, 2004, doi: 10.1016/j.apor.2004.08.002.

[40] O. Yaakob, F. Ellyza, K. Mohd, A. Hassan, and K. King, "Satellite-based wave data and wave energy resource assessment for South China Sea," *Renew. Energy*, vol. 88, pp. 359–371, 2016, doi: 10.1016/j.renene.2015.11.039.

[41] Y. Lin, S. Dong, Z. Wang, and C. G. Soares, "Wave energy assessment in the China adjacent seas on the basis of a 20-year SWAN simulation with unstructured grids," *Renew. Energy*, vol. 136, pp. 275–295, 2019, doi: 10.1016/j.renene.2019.01.011.

[42] D. Zhang, W. Li, and Y. Lin, "Wave energy in China : Current status and perspectives," *Renew. Energy*, vol. 34, no. 10, pp. 2089–2092, 2009, doi: 10.1016/j.renene.2009.03.014.

[43] M. M. Amrutha and V. S. Kumar, "Changes in Wave Energy in the Shelf Seas of India during the Last 40 Years Based on ERA5 Reanalysis Data," pp. 1–23, 2020.

[44] S. V Samiksha, P. Vethamony, W. E. Rogers, P. S. Pednekar, M. T. Babu, and P. K.

D. Kumar, “Wave energy dissipation due to mudbanks formed off southwest coast of India,” *Estuar. Coast. Shelf Sci.*, 2017, doi: 10.1016/j.ecss.2017.07.018.

[45] G. Bracco, M. Canale, and V. Cerone, “Control Engineering Practice Optimizing energy production of an Inertial Sea Wave Energy Converter via Model Predictive Control,” *Control Eng. Pract.*, vol. 96, no. May 2019, p. 104299, 2020, doi: 10.1016/j.conengprac.2020.104299.

[46] C. Xu and Z. Huang, “A dual-functional wave-power plant for wave-energy extraction and shore protection: A wave-flume study,” *Appl. Energy*, vol. 229, no. March, pp. 963–976, 2018, doi: 10.1016/j.apenergy.2018.08.005.

Appendix A: Data Collection

Australia[38]

Table 1
Geometry details of simulated point absorber WEC.

Variable	Value	Unit
Water Depth	50.0	m

Table 2
Sea state parameters used in the hydrodynamic analysis of point absorber WEC.

Sea state Number	1	2	3	4	5	6	7	8	9	10	11	12
Significant Wave Height, H_s (m)	0.75	1.25	1.75	2.25	2.75	3.25	3.75	4.25	4.75	5.25	5.75	6.25
Zero Crossing Wave Period, T_z (s)	4.0	5.0	6.0	7.0	7.0	8.0	9.0	9.0	9.0	10.0	11.0	12.0

Italy[45]

Water depth	32 m

Table 3
Wave profiles caharacteristics.

Wave ID	T_e (s)	H_s (m)	P_s (kW m^{-1})	f_o (%)
1	5.31	1.18	3.65	11.5
2	6.44	1.97	12.25	12.2
3	7.38	0.67	1.61	6.5
4	6.54	0.68	1.50	16.2
5	6.83	1.36	6.23	10.8
6	8.09	2.20	19.18	2.2
7	7.77	1.45	8.06	5.3
8	7.27	1.99	14.16	7.5
9	5.36	0.69	1.25	27.8

Belgium[39]

Table 1
Selected spectra: Akkaert Bank (water depth 22 m), wind sector 6 (SW)

H_s class	1	2	3	4	5	6	7	8	9
H_s (m)	0.0–0.5	0.5–1.0	1.0–1.5	1.5–2.0	2.0–2.5	2.5–3.0	3.0–3.5	3.5–4.0	4.0–4.5
T_z (s)	2.5–3.5	3.5–4.5	3.5–4.5	3.5–4.5	4.5–5.5	4.5–5.5	5.5–6.5	5.5–6.5	5.5–6.5
Occurrence (%)	0.78	1.74	50.43	28.50	13.29	3.63	1.10	0.49	0.02

China[41][42]

Table 2
Fundamental characteristics of the 17 hotspots picked out.

Ref	Abbr.	Regions	Water Depth		Distance to shore [km]	Average Wave Energy Flux [KW/m]	Monthly Variability Index	Exploitable Occurrences [%]	OHI	Lon. [Degree]	Lat. [Degree]
			Condition	Value [m]							
1	Z. O	Zhejiang	offshore	50.85	20.59	5.852	1.143	56.0	2.868	122.92E	30.01N
2	Z. N		nearshore	23.21	17.78	5.024	0.969	55.9	2.895	121.82E	28.13N
3	Z. M		medium	48.28	19.98	6.084	0.997	59.2	3.616	122.08E	28.33N
4	F. N	Fujian	nearshore	24.36	8.00	6.598	1.377	60.8	2.915	119.96E	25.36N
5	F. M		medium	47.69	24.52	8.671	1.457	64.9	3.863	120.12E	25.30N
6	F. O		offshore	68.44	21.19	8.051	1.441	63.4	3.541	119.94E	25.20N
7	G. N	Guangdong	nearshore	23.00	20.72	5.362	1.503	54.7	1.949	117.49E	23.26N
8	G. M		medium	34.19	23.24	5.490	1.401	57.8	2.266	116.59E	22.75N
9	G. O		offshore	51.59	19.10	5.405	1.474	59.3	2.176	114.16E	21.75N
10	H. N	Hainan	nearshore	22.71	10.15	5.910	2.172	54.2	1.475	111.11E	19.95N
11	H. M		medium	40.32	15.47	6.475	2.113	57.7	1.767	111.30E	19.94N
12	H. O		offshore	83.14	22.53	6.993	2.131	58.8	1.929	111.47E	19.94N
13	T. M	Taiwan	medium	47.13	9.43	6.351	1.706	53.3	1.985	121.07E	25.13N
14	T. O		offshore	154.91	18.36	9.933	1.473	66.7	4.498	122.00E	25.23N
15	X. O	Xisha	offshore	57.21	3.93	9.233	2.531	60.4	2.202	112.61E	16.59N
16	X. P	Penghu	offshore	62.03	22.04	10.543	1.838	58.6	3.361	119.41E	23.86N
17	O. N	Orchid	nearshore	13.44	6.26	9.528	1.610	68.4	4.050	121.53E	22.11N

Hotspot	H_s [m]		T_e [s]		J [KW/m]	
	Operational	High	Operational	High	Operational	High
Z. O	0–2.1	2.1–3.5	0–6.7	6.7–8.7	0–13.7	13.7–49.7
Z. M	0–2.1	2.1–3.5	0–6.6	6.6–8.8	0–13.9	13.9–47.0
F. M	0–2.7	2.7–3.8	0–6.9	6.9–8.3	0–23.4	23.4–55.2
G. N	0–2.2	2.2–3.1	0–6.3	6.3–7.5	0–14.3	14.3–33.4
G. M	0–2.1	2.1–3.1	0–6.4	6.4–7.7	0–13.8	13.8–33.8
G. O	0–2.0	2.0–2.9	0–6.9	6.9–8.2	0–13.0	13.0–31.4
H. O	0–2.4	2.4–3.4	0–7.3	7.3–8.5	0–19.0	19.0–45.1
T. M	0–2.4	2.4–3.4	0–7.2	7.2–8.7	0–17.8	17.8–46.2
T. O	0–2.6	2.6–4.2	0–7.5	7.5–9.4	0–25.0	25.0–78.0
X. O	0–2.7	2.7–4.0	0–7.7	7.7–9.1	0–25.9	25.9–70.1
P. O	0–3.0	3.0–4.4	0–7.1	7.1–8.3	0–31.0	31.1–75.7
O. N	0–2.7	2.7–4.1	0–7.5	7.5–9.0	0–25.6	25.6–66.6

India[43][44]

Location	Geographic Position	Significant Wave Height, H_s (m)	Mean Wave Period, T_e (s)	Wave Power (kW/m)	Water Depth (m)	Distance from the Coast (km)	Wave Length (m)	Wave Power Trend (kW/year)
1	22.50° N; 68.25° E	1.3	7.2	9.75	63	83	80.9	0.027
2	21.00° N; 69.50° E	1.4	7.5	11.00	65	54	87.8	0.027
3	19.50° N; 71.25° E	1.4	7.0	9.77	75	140	76.5	0.021
4	18.00° N; 72.00° E	1.4	7.5	10.58	47	104	87.6	0.019
5	16.50° N; 72.75° E	1.4	7.6	10.37	68	60	90.2	0.020
6	15.00° N; 73.50° E	1.3	7.2	8.89	75	45	80.9	0.016
7	13.50° N; 73.50° E	1.4	7.7	10.21	80	122	92.6	0.027
8	12.00° N; 74.50° E	1.2	7.9	7.75	129	71	97.4	0.020
9	10.50° N; 75.50° E	1.0	7.9	6.49	100	54	97.4	0.017
10	09.00° N; 76.00° E	1.3	8.4	8.35	90	52	110.2	0.031
11	07.75° N; 77.25° E	1.5	7.8	10.35	61	42	94.9	0.037
12	08.25° N; 78.25° E	1.3	7.3	6.22	28	24	81.1	0.017
13	10.50° N; 80.25° E	0.9	5.0	2.29	104	43	39.0	0.009
14	12.00° N; 80.00° E	0.9	5.7	2.47	27	14	50.6	0.011
15	13.50° N; 80.50° E	0.9	6.1	2.91	90	21	58.1	0.013
16	15.00° N, 80.25° E	0.8	5.9	2.28	49	21	54.4	0.005
17	16.75° N, 82.50° E	1.0	6.8	3.97	99	16	72.2	0.014
18	18.50° N; 84.50° E	1.2	7.5	6.00	41	17	87.3	0.026
19	20.00° N; 86.75° E	1.2	7.9	6.60	58	30	97.3	0.021
20	21.00° N; 89.00° E	1.3	8.5	8.80	75	70	112.8	0.019

Appendix B: MatLab Code

```
clear; clc
Water_depth = input('water depth: ');%Water depth
w_period = input('wave period: ');%Wave Period
w_height = input('Significant wave Height: ');%Significant wave Height
g = 9.81;%gravity
L=(((4*(pi^2)*Water_depth)/((w_period^2)*g))*(coth((2*pi*sqrt(Water_depth
))/(w_period*sqrt(g)))^(3/2))^(2/3))^(-1)*2*pi*Water_depth;%Wave length
gamma = 0.9;% Dimensionless restoring force
zeta = 0.35;% Dimensionless damping ratio
syms s %Dimensionless frequency
DispEq = gamma*(s^4)*tanh(mu)+1i*mu*gamma*zeta*(s^3)-mu*(s^2)-
1i*(mu^2)*gamma*zeta*s*tanh(mu)+(mu^2)*(1-gamma)*tanh(mu)==0;
sigma= double(solve(DispEq,s));
max_sigma = sigma(1); %initialize
for index = 1:length(sigma)
    if real(sigma(index)) > real(max_sigma)
        max_sigma = sigma(index);
    end
end

Re_max_sigma = real(max_sigma);
Im_max_sigma = imag(max_sigma);

alpha = ((cosh(mu))^2)*(1-((mu*tanh(mu))/(Re_max_sigma)^2));
%Dimensionless amplitude ratio of bottom to surface
Dd = 0.5*(((sinh(2*mu))/2)*((Re_max_sigma^2/mu)+(mu/Re_max_sigma^2))-
2*(sinh(mu))^2)+((1-alpha)/2)+(alpha/(2*gamma)); %Dimensionless constant
tau = w_period*sqrt(g/w_height);

E = 0.5*exp(2*Im_max_sigma*tau)*Dd;%Energy in dimensionless form
E_carpet = 0.5*rho*g*((a_s)^2)*E*A_c;%The energy in the carpet for one
period of time
fprintf('Energy=%f\n',E_carpet);
```